NAL PROPOSAL No. 198

Scientific Spokesman:

S. Olsen
Department of Physics
University of Rochester
Rochester, New York 14527

FTS/Off-net: 716 546-4900
275-4394

A proposal for a Magnetic Recoil Spectrometer for the Gas Jet Target

D. Nitz, M. Miller, S. L. Olsen and D. A. Gross

The University of Rochester
Rochester, N. Y. 14527

K. Abe, J. Alspector, K. Cohen, J. Mueller, B. Robinson and F. Sannes

Rutgers University
New Brunswick, N. J. 08903

December 21, 1972

A proposal for a Magnetic Recoil Spectrometer for the Gas Jet Target

D. Nitz, M. Miller, S. L. Olsen and D. A. Gross
The University of Rochester
Rochester, N. Y. 14527

K. Abe, J. Alspector, K. Cohen, J. Mueller, B. Robinson and F. Sannes
Rutgers University
New Brunswick, N. J. 08903

Abstract

We propose to measure recoils from the internal H_2 and D_2 gas jet target at values of $|t|$ up to 2 GeV^2 using a small single-magnet spectrometer. The wide range of incident energies available at the internal target is well suited for the study of the s dependence in pp elastic and inelastic scattering as well as elastic and coherent inelastic p-d scattering.

Scientific Spokesman: Stephen Olsen
716-275-4394
NAL ext. 3795

I. Introduction

We propose to measure the s dependence of elastic and inelastic p-p and p-d scattering, at t values ranging up to t $\simeq$-2.0 $(GeV/c)^2$. The basic idea is to use a small, single magnet, high resolution spectrometer and look at recoils from the gas jet target. The use of a magnet will allow measurements at higher values of t than are accessible in the current recoil experiments at CØ, greatly enhancing the usefulness of the gas jet. The unique ability of the internal target to span the entire energy range in the main ring greatly facilitates the study of the generally slow variations with s, characteristic of high energy scattering. The primary physics questions addressed by this experiment are, for elastic p-p scattering:

1) Does shrinkage persist at high t?
2) Does the break seen at t $\simeq$-1.2 $(GeV/c)^2$ at 24 GeV develop into a dip? If so, how fast? Does it move as s increases?
3) What is the s dependence of $d\sigma/dt$ for t's beyond the break (dip)?

for inelastic scattering:

1) What is the s and x dependence of the inclusive proton spectrum for large values of t
2) How does the production of the N* (1520) and N* (1688) as a function of s and t, compare with elastic scattering.

and for p-d scattering:

1) How do coherent inelastic processes on deuterium compare with elastic p d scattering for $|t| \geq .2$ $(GeV/c)^2$?

The investigation of the questions concerning elastic scattering requires an understanding of the inelastics, making it advantageous to study them simultaneously.

We summarize the reasons which make this proposed experiment well suited for the investigation of these questions:

a) The internal target laboratory allows for the widest accessible variation in s. No special provisions are necessary to accept whatever energy the machine may attain.

b) The recoil kinematics for elastic scattering are insensitive to the incident energy.

c) The t resolution would be quite high, enabling us to investigate the possibility of quite narrow structures in t.

d) These investigations would cause little interference with the general program of the laboratory.

II. Motivation

1) Proton-Proton Elastic Scattering

The shrinkage of the forward peak in p-p elastic scattering, as seen in experiment 36, is generally interpreted as an increase in the interaction radius of the proton[1]. On the other hand, some models interpret this sharpening of the peak as being due to the further blackening of a constant area interaction region[2,3]. The break in $d\sigma/dt$ observed at $t \approx -1.2$ $(Gev/c)^2$ at 24 Gev[4] is interpreted as the first diffraction minimum which is filled by the real part of the scattering amplitude, i.e., the proton is still quite grey at these energies. As the position of this diffraction minimum also reflects the radius of the interaction region, measuring how this break (dip) moves with s will be a good test between the two types of models.

In the near future, experiment 36 will have a precision measurement of the "blackness" of the proton over the s range available at NAL. It would be interesting to study the rate at which the break forms into a dip over this same energy region. Recent ISR results[5] at

1500 Gev, indicate that a dip has indeed formed at a t $\simeq$-1.3 $(GeV/c)^2$ (See fig 1) indicating a preference for the second type of model i.e. those with a constant area of interaction. One of these models, the impact picture of Cheng, Walker, and Wu[3], predicts a slow increase in $d\sigma/dt$ with s, for t values beyond the break and for s above 100 Gev. One of the primary motivations for this experiment is the test of this striking prediction.

2) The Inclusive Proton Sprectrum

The study of the inclusive proto[illegible]um as a function of s,t and M^2 will provide very useful tests of present Regge parametrizations for this reaction. In particular we will be able to extract effective Regge trajectories from the data and study the t dependence of triple Regge couplings. For large values of t one may expect cut contributions to become important, thus leading to a flattening of the effective trajectories. Independently of any specific model however, the study of the inclusive proton spectrum is complementary to that of pp elastic and we can expect to observe related dip structures in $\frac{d\sigma}{dt}$. This experiment is unique in that it will span continuously a large region of s and M^2 as shown in figure 2.

3) N* (1520) and N* (1688) Production

It would be interesting to compare the s and t dependence for N* (1520) and N* (1688) production with elastic scattering. If the production of these resonances and elastic scattering proceeds via the same diffractive mechanism, the features of elastic scattering at every s should be reflected in the production of these isobars. While it would be difficult to resolve the N* (1520) from the N* (1688) in the high s region, we could resolve them at low s and measure the sum of the two channels at high s.

4) Coherent Deuteron Interactions

Coherent deuteron processes are primarily interesting because they enhance diffractive channels. Experiment 186 will measure recoil deuterons at small $|t|$ ($\leq .1$ (Gev/c)^2) in order to study diffractive dissociation. Glauber theory relates processes happening in the "double scattering" region ($|t| \geq .25$ (Gev/c)^2) to the single particle processes at $t/4$, i.e. just that region covered in experiment 186. In the Glauber model, with this as input, the coherent inelastic processes in the double scattering region and in the interference region between single and double scattering (i.e. $|t| \geq .25$ (Gev/c)^2) are a means for studying the gross features of such exotic processes as forward N*-nucleon elastic scattering. Even rather coarse measurements of forward elastic scattering of N*'s would be very useful for determining whether or not these are composite particles. Extracting such information is complicated both by poorly understood ground state deuterium properties as well as off the mass shell effects[7]. Comparison of the inelastic to elastic scattering, and making measurements at both low and high energies can reduce these uncertanties.

III. Experimental Considerations

1) Resolution requirements

The technique proposed is a single arm spectrometer and thus employs the missing mass technique. The mass resolution varies inversely with the beam momentum so a successful experiment at high energies requires good resoltuion. In principle, in order to isolate elastic scattering from inelastic scattering, a mass resolution of one pion mass is required. In practice one can get by with resolving elastic scattering from the closest structure in the mass spectrum. Mass spectra in this t region have been measured at 24 GeV by Allaby et al[4] and are shown in fig. 3. The first structure seen above t=-.4 $(Gev/c)^2$ is the N* (1520). To resolve elastic scattering one thus needs a mass resolution somewhat better than 0.5 Gev/c^2.

The angular resolution required for a mass resolution Δm is

$$\Delta\theta = \frac{m\Delta m}{P_o\sqrt{|t|}}$$

where P_o is the incident beam momentum. For Δm = .5 Gev/c^2, P_o = 500 Gev/c and $|t|$ = 1 $(Gev/c)^2$ an angular resolution of 1 mrad is required. The energy resolution required is

$$\frac{\Delta T}{T} = \frac{4m^2\Delta m}{P_o|t|}$$

where T is the recoil kinetic energy. Again at 500 Gev, $|t|$=1 $(Gev/c)^2$ and Δm= .5 Gev/c^2 an energy resolution of 0.4% is required. This corresponds to a momentum resolution of .3% or, for a 20° bend, a determination of the bend to 1 mrad. An apparatus that determines

angles to better than 1 mrad is required. The resolution requirements for the coherent deuteron measurements are somewhat less stringent since the t values of interest are about a factor of five lower.

2) Backgrounds

We have two types of background to contend with. First there is the target associated background consisting mainly of π's and K's produced in the gas jet. Second there is room background primarily due to the scattering of the beam in the residual gas from the jet. We will discuss these separately.

i) Target Associated Backgrounds

To estimate typical K and π fluxes from the target we consider 200 Gev pp elastic scattering at $t = -1.2$ $(\text{Gev/c})^2$. The value of X for these protons is $\simeq .9$. For π^+'s at the same angle and momentum $X \simeq .6$ and for K^+'s $X \simeq .7$. At 24 Gev, for these values of X and $P_\perp$, the ratios of the invariant cross sections for the three particles are roughly[4] (see Fig. 4)

$$E\frac{d\sigma}{dp^3}\Big|_{pp\to px} : E\frac{d\sigma}{dp^3}\Big|_{pp\to\pi^+x} : E\frac{d\sigma}{dp^3}\Big|_{pp\to K^+x} \simeq 50:3:1.$$

The large predominance of protons is due to the fact that elastic scattering occurs near the kinematic boundary for π's and K's. It is expected that these invariant cross sections vary slowly or not at all with s, so we don't expect much contamination near the elastic scattering region. On the other hand, for more inelastic events, the situation is not as favorable. For protons emitted with half the momentum of the elastic recoil, $X \simeq .8$. For π's and K's at the same angle and momentum $X \simeq .3$ and $\simeq .5$ respectively. Here the ratios of the invariant cross sections are (again roughly)

$$p: \pi: K \simeq 50: 30: 1.$$

In this region particle identification is necessary. Here the protons are slow, $\beta \simeq .5$, and have a flight time over a 3 meter apparatus which is 4 nanoseconds longer than that of a π, so protons and π's could thus be distinguished by measuring time of flight using the machine RF structure. Also these protons would be below the threshold of a lucite Čherenkov counter. Thus, there are two handles for particle identification where it is necessary. The deuterons will be quite distinctive, their $\beta \simeq .3$. Comparing time of flight to momentum measurements will uniquely identify them.

ii) Room Background

We have measured the instantaneous singles rate in a 50 cm^2 counter, about 2 meters from the beam pipe with $\sim 10^{10}$ protons per booster pulse, to be ~.3 megacycles. We could attribute most of these particles to beam interactions in the residual gas, produced by the gas jet, in the upstream beam pipe. Soon the accelerator will operate with perhaps 100 times as much beam in a booster pulse, at which time we can expect instantaneous background radiation of ~.5 megacycles/cm^2. For this experiment we plan to sacrifice solid angle and use a small detection apparatus made up of elements with areas not exceeding a few cm^2. In this way the rates in the scintillators could be kept below a megacycle even for a circulating beam of 10^{12}/booster pulse. The precision spatial measurements will be done by small proportional wire planes where each wire covers ~ 1 cm^2 of area, keeping the rates per wire below 1 megacycle.

At the current time an effort is underway to reduce the quantity of residual gas going into the upstream beam pipe by revising the vacuum system. If this is successful it will be an obvious benefit, but in any case we will prepare for the worst case conditions.

IV. Experimental Apparatus

1) Hardware

We propose to decouple the measurement of scattering angle from the momentum measurement by using the magnet to bend vertically. We need a $B \cdot \ell$ of 15 kilogauss meters with a gap of 5 to 10 cm along the field lines and 15 cm across. This magnet would be mounted on an arm which would pivot about the target point. (See Figure 5). The jet will be viewed from 50° to 80°, through a thin titanium window. The space from the target window to the magnet entrance would be about 1 meter and in this space we would have 1 horizontal and 2 vertical proportional wire planes (PWP) covering 5 cm horizontally and 7.5 cm vertically, with wire spacing of 1.5 mm. Behind we would have 3 vertical chambers and two horizontal chambers ranging in size from 7.5 cm x 15 cm to 10 cm x 30 cm again with 1.5 mm wire spacing. The total number of wires will be $\sim$550 for the momentum measurement and $\sim$150 for the scattering angle measurement. The vertical wire planes together with the small vertical dimension of the beam at high energies ($\lesssim$ 2 mm) should give a bending angle measurement to an accuracy of $\sim$1 mrad. The scattering angle measurement will be limited by multiple scattering. For this reason the amount of material in the spectrometer will be kept to a minimum. At the window to the vacuum chamber we will have a thin ($\lesssim$1 mm thick) scintillator for triggering. Behind the last PWP's will be a scintillation hodoscope for the trigger, a rough angular measurement, and for the time of flight determination. Following that will be lucite Čherenkov counters for fast particle identification. In all the drift spaces will be vacuum pipes with thin mylar windows to minimize multiple scattering. After a trigger the wires

will be read-out and the time of the count in the rear hodoscope relative to the machine RF will be determined. These data will be accumulated by a PDP-8 computer and written on tape between jet bursts.

2) Trigger

The trigger must pick out particles originating from beam - gas jet collisions. It is our experience that the room background is highly correlated with the machine RF structure and including a gate generated from the RF into the fast coincidence eliminates this room background effect from the trigger.

3) Monitoring

To study variations with s,measurements made at different times and under different conditions have to be related. Therefore it is critical to have an effective monitor of the beam on target. While there is a good possibility that a monitor may be devised using delta rays from the gas or using ionization or flourescence measurements we could have an adequate (≈5%) monitor independent of the success of these other methods. Figure 6 shows a pulse height distribution in a solid state detector mounted in the vacuum system and viewing the jet at an angle of 86° from the beam line. The peak corresponding to elastic p-p scattering is clear and has very little background under it. The s dependence of the total cross-section, the slope parameter and the real part of the forward amplitude are well enough known to relate the elastic counts at fixed t to beam on target to ~5%. The quality of this monitor will improve with further total cross section measurements.

4) Operating Inside the Main Ring

We are familiar with the problems associated with operating inside the main ring, in particular the limited access available for maintenance of equipment. We plan to modularize the detection apparatus so that defective units can be replaced rather than repaired in place. Keeping the apparatus small in scale greatly facilitates this.

3) Rates

i) pp elastic scattering

ISR results (Fig. 1) give $d\sigma/dt$ between 10^{-32} and 10^{-31} $cm^2/(Gev/c)^2$ for $|t|>1.0$ Gev at 1500 Gev. For a solid angle 5 cm horizontal and 15 cm vertical at a distance of 2 meters we have, for recoils at 60° ($t\approx 1.0$ $(Gev/c)^2$);

$$\Delta\phi = .15m/\ (2.0\ m \times SIN\ 60° \times 2\pi) = .015$$

$$\Delta t = 4m\sqrt{t}\ \Delta\theta = 4 \times 1 \times 1 \times \frac{.05}{2.0} = .1\ (Gev/c)^2$$

For 5×10^{12} protons/pulse, a jet with density 2×10^{-7} gms/cm^2, .3 seconds in duration and $d\sigma/dt = 10^{-31}$ cm^2 $(Gev/c)^2$ we expect an elastic event rate of

5×10^{12} prot $\times$ 5×10^{4} circ/sec $\times$ 6×10^{23} targ/gm $\times$ 2×10^{-7} gm/cm^2 $\times$
$\times$ 10^{-31} cm^2/(Gev/c)^2 $\times$ .1 (Gev/c)^2 $\times$ .3 sec $\times$ .015 ($\Delta\Omega$)

$\approx$1.4 events/jet burst.

This corresponds to ~1000 events per jet burst per hour which is adequate for the purposes of these investigations.

ii) pp inclusive scattering

The invariant cross section $sd^2\sigma/dtdM^2$ at $t = -0.5$ $(GeV/c)^2$ and $s = 400$ GeV^2 is 10 mb/GeV^2 (Exp. 67). With the above geometry this gives a counting rate of

$$N_b N_t \frac{1}{\pi}\frac{p_3^2}{E_3}\frac{s\,d^2\sigma}{dt\,dM^2} = 2.5\times10^{17} \times 1.2\times10^{17} \times \frac{1}{\pi} \times \frac{0.5}{1.2} \times 10^{-26}$$
$$\times\ 2\times10^{-3} \times 5\times10^{-2} \times 0.3$$

= 1200 events/jet burst

iii) pd elastic scattering

at $t\approx-.25$ $(Gev/c)^2$ we estimate from 24 Gev data[8] that $d\sigma/dt$ will be about 2×10^{-29} $cm^2/(Gev/c)^2$. $\Delta\phi$ is, of course, the same, $\Delta t \approx .1$ $(Gev/c)^2$, the jet is more dense ~ 10^{-6} gms/cm^2 so we expect an elastic event rate of

5×10^{12} prot $\times$ 5×10^{4} circ/sec $\times$ 3×10^{23} targ/gm $\times$ 10^{-6} gm/cm^2 $\times$
$\times$ 2×10^{-29} cm^2/(Gev/c)^2 $\times$ .1 (Gev/c)^2 $\times$ .3 sec $\times$ .015

$\approx$675 events/jet burst.

V. Procedure

After the installation of the equipment we would need about two weeks of running for tuning and debugging. Since the resolution requirements for the coherent deuteron and the inclusive proton measurements are less stringent and since the event rates are higher we would study these first. This should take two weeks with at least two jets per pulse. For elastic p-p scattering we could run 6 to 8 t positions at 10 energies in a week. These measurements would indicate the position of the break as a function of energy. We would then study this region carefully for another week. We therefore ask for 6 weeks of running at the highest machine energy with 2 or 3 jets per cycle.

VI. Other Experiments

An extensive program for hadron scattering in this t range is planned for the meson laboratory. These experiments will study $\pi^{\pm}$,$K^{\pm}$ and $p^{\pm}$ scattering for a wide range of t values and for energies up to 200-300 Gev. Our experiment could not match these experiments in terms of t range or in the variety of the incident particles. We will span a wider range in s, however, from $s = 15$ to $s \simeq 940$ Gev^2, overlapping both AGS and ISR measurements.

The ISR results on pp elastic scattering, referred to in this proposal, were a motivation for this proposal. We are particularly interested in seeing how the dip seen at 1500 Gev forms and moves as a function of energy. Our t resolution will be about ten times better, enabling us to study the depth and position of this structure with more precision.

VII. Details

1) Timetable

We could start on the procurement and the construction of the apparatus immediately. We have commitments for experiments 186 and 188, but we could install this apparatus soon after their completion which would most likely be July or August 1973.

2) Manpower

We could have 2 or 3 PhD physicists and some students in residence at NAL. Others can be here during the summer for installation and start up, and subsequently for runs. The possibility exists for extending the collaboration to one more institution or to other interested individuals.

3) Equipment

We would provide the proportional wire planes and their readout electronics, the scintillation hodoscopes and a PDP-8 computer. We would expect NAL to provide facilities for the magnet and to operate the gas jet target. Magnets similar to what we need exist at cyclotron laboratories and we are currently looking into the possibility of borrowing one for this experiment. If not, with NAL's assistance, we could build one.

4) BØ and Beyond

The experiment described in this proposal has been designed for the present internal target facility at CØ. The proposed laboratory at BØ would allow us to make the lever arms for the angle measurements, before and after the magnet, 2 or 3 times longer, giving better mass resolution. This would simplify the separation of elastic scattering events, particularly at 400 and 500 Gev. The longer lever arms would also make the apparatus suitable for studying these reactions at the even higher energies which could be available with the energy doubler.

1) For a review of the many theoretical models for pp elastic scattering see:
J. D. Jackson, Rev. Mod. Phys. 42 (1970) 12.

2) For example: Tse Yuen Cheng, Shu Yuan Chu and Archibald W. Hendry. "A Unified Picture of Proton-Proton Elastic Scattering from 3 to 24 Gev/c". Indiana University preprint COO-2009-33, 1972.

3) H. Cheng, J. K. Walker, and T.T. Wu. "Impact Picture of Very-High-Energy Hadron Interactions (With Numerical Results)" MIT preprint 72-3477.

4) J. V. Allaby et al, Cern Rome Collaboration report at the Fourth International Conference on High Energy Collisions, Oxford, England (April, 1972).

5) C. Rubbia et. al., Talk presented during the parallel sessions of the XVI International Conference on High Energy Physics, Batavia, 6-13 September 1972.

6) R. J. Glauber, Proceedings of the Third International Conference on High Energy Physics and Nuclear Structure, New York, N. Y. 1969, edited by S. Devons (Plenum, New York, 1970) pg. 207.

7) L. Van Hove, Nucl. Phys. B46 (1972) 75 and, Alfred S. Goldhaber SUNY preprint.

8) U. Amaldi et al. Nucl.Phys. B39 (1972) 39.

Figure 1: Proton-Proton elastic scattering measurements from 3 Gev up to 1500 Gev. The t resolution for the 1500 Gev data is shown together with an optical model calculation for a "black" proton.

Figure 2: A map of the s and M^2 region of the inclusive proton spectrum which will be explored in this experiment. The vertical lines (fixed S)-are regions covered at the ISR and lower energy machines. The sloped lines indicate the points measured in experiment 67 at NAL.

Figure 3: The missing mass distribution seen at 24 Gev by Allaby et al[4]. Above $|t|=\cdot 0.4$ $(Gev/c)^2$ the structure nearest the elastic peak is the N* (1520).

Figure 4: The invariant cross sections at 24 Gev for p's. k^+'s and π^+'s, taken from reference 4.

Figure 5: a) An elevation view of the proposed apparatus. The detailed configuration depends upon the actual dimensions of the magnet. b) A plan view showing how the spectrometer fits into the tunnel.

Figure 6: A recoil proton energy spectrum measured in a 1 mm thick surface barrier detector, 86° from the beam line. The peak at 10 Mev corresponds to elastic p-p scattering at $t=-.02$ $(Gev/c)^2$.

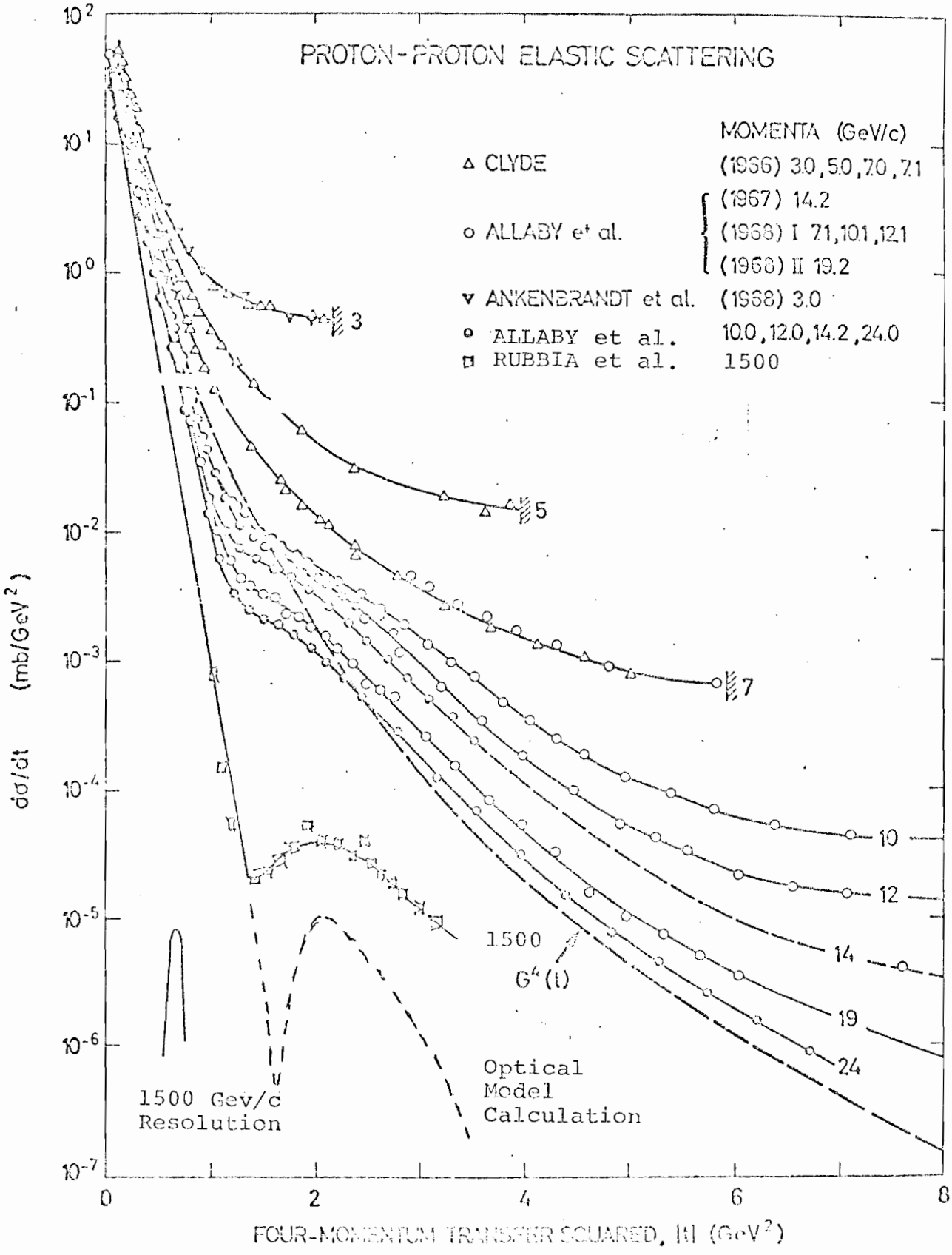
PROTON-PROTON ELASTIC SCATTERING
MOMENTA (GeV/c)
△ CLYDE (1966) 3.0, 5.0, 7.0, 7.1
(1967) 14.2
o ALLABY et al. (1968) I 7.1, 10.1, 12.1
(1968) II 19.2
▽ ANKENBRANDT et al. (1968) 3.0
o ALLABY et al. 10.0, 12.0, 14.2, 24.0
□ RUBBIA et al. 1500
3
5
7
10
12
14
19
24
1500
G⁴(t)
Optical Model Calculation
1500 Gev/c Resolution
dσ/dt (mb/Gev²)
FOUR-MOMENTUM TRANSFER SQUARED, |t| (GeV²)

FIGURE I

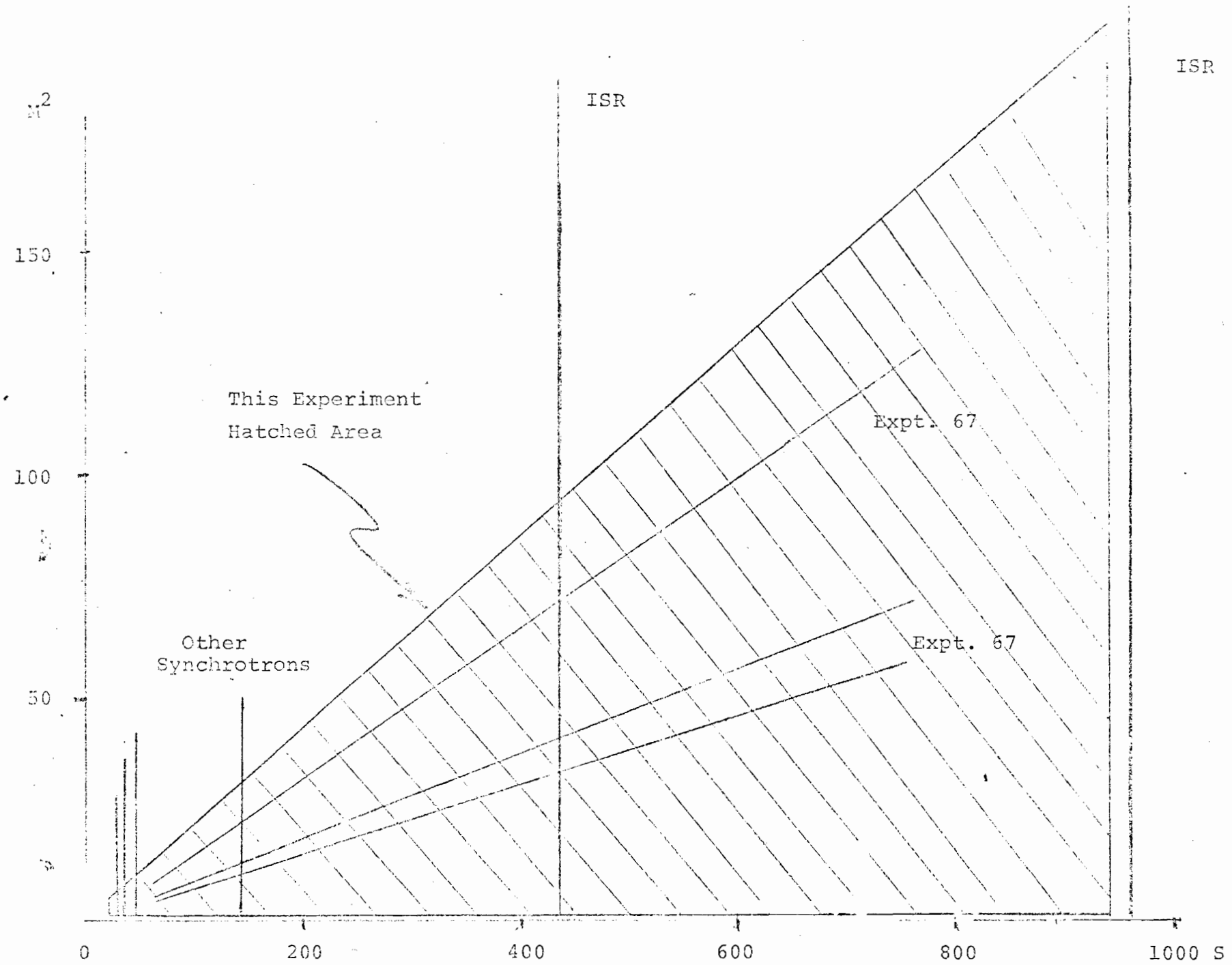
ISR
ISR
150
100
50
This Experiment
Hatched Area
Expt. 67
Expt. 67
Other
Synchrotrons
0
200
400
600
800
1000 S

FIGURE 2

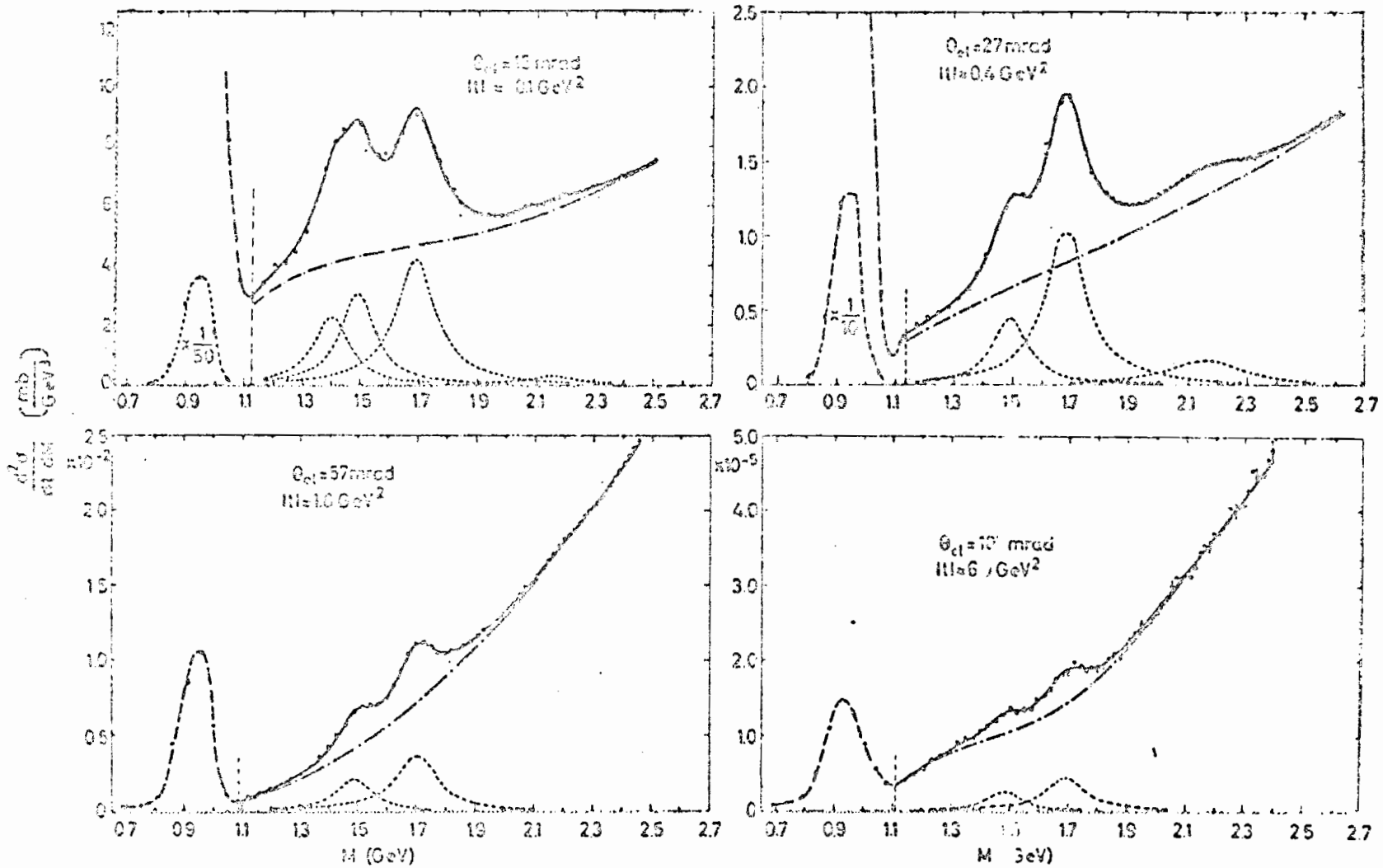
pp → pX
P_{LMC} = 24 GeV/c
$\frac{d^2\sigma}{dt\,dM}$ $\left(\frac{mb}{GeV^2}\right)$
θ_{el}=15 mrad
|t|= 0.1 GeV²
θ_{el}=27mrad
|t|=0.4 GeV²
θ_{el}=57mrad
|t|=1.0 GeV²
θ_{el}=10' mrad
|t|=6 /GeV²
M (GeV)
M GeV)

FIGURE 3

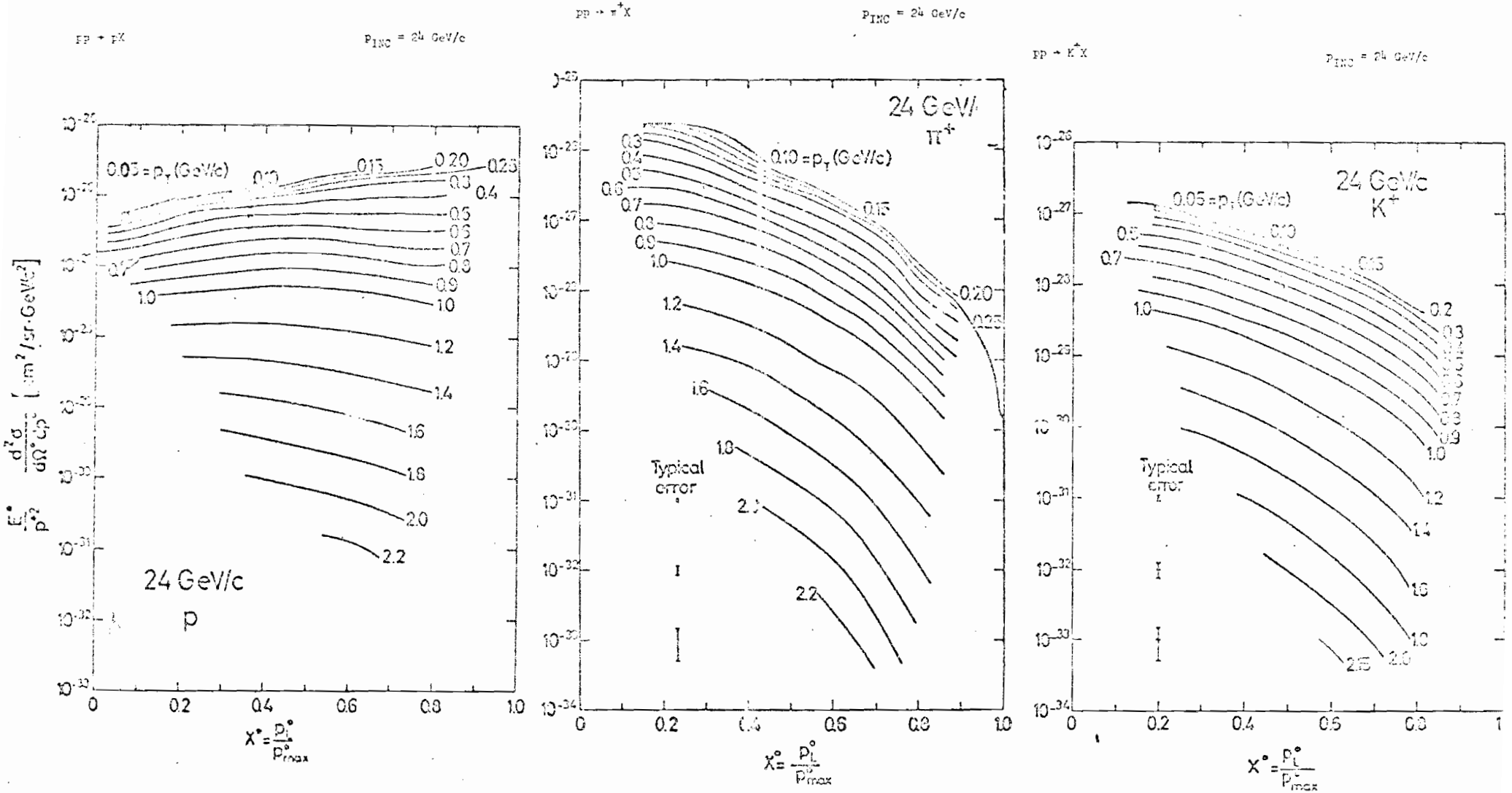
pp → pX
P_INC = 24 GeV/c
0.05 = p_T (GeV/c)
0.10
0.15
0.20
0.25
0.3
0.4
0.5
0.6
0.7
0.8
0.9
1.0
1.2
1.4
1.6
1.8
2.0
2.2
24 GeV/c
p
pp → π⁺X
P_INC = 24 GeV/c
24 GeV/c
π⁺
0.10 = p_T (GeV/c)
Typical error
pp → K⁺X
P_INC = 24 GeV/c
24 GeV/c
K⁺
0.05 = p_T (GeV/c)
Typical error
E* d³σ/dp*³ [cm²/sr·GeV⁻²]
X* = p_L*/p*_max
X° = p_L°/p°_max

FIGURE 4

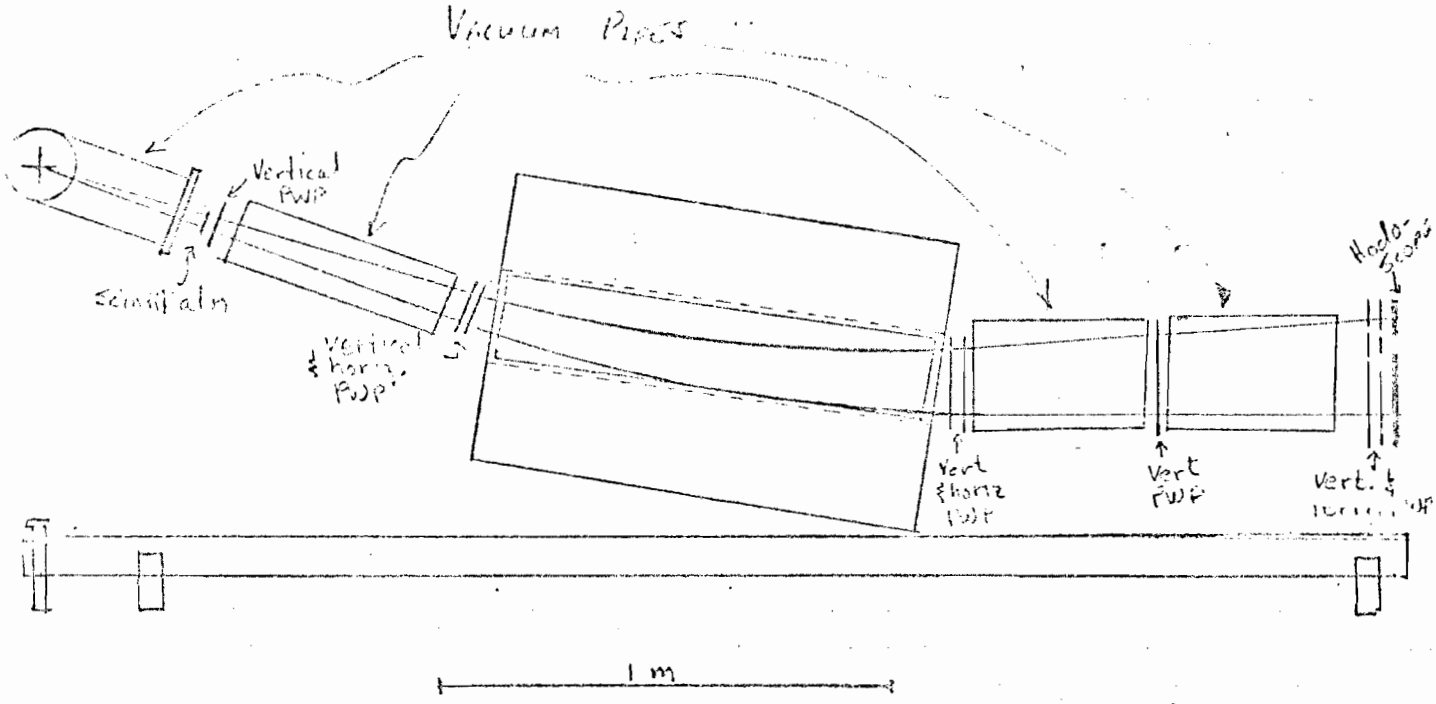

FIGURE 5a

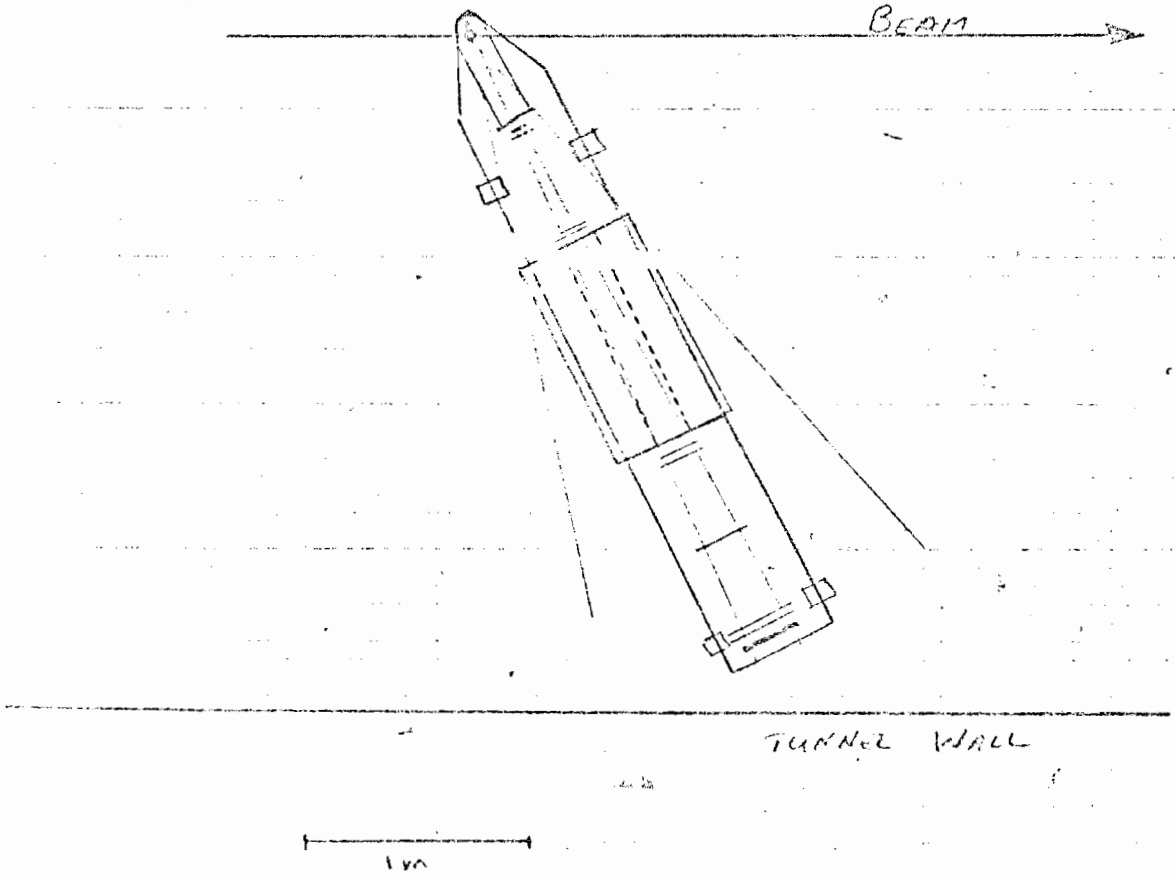

FIGURE 5b

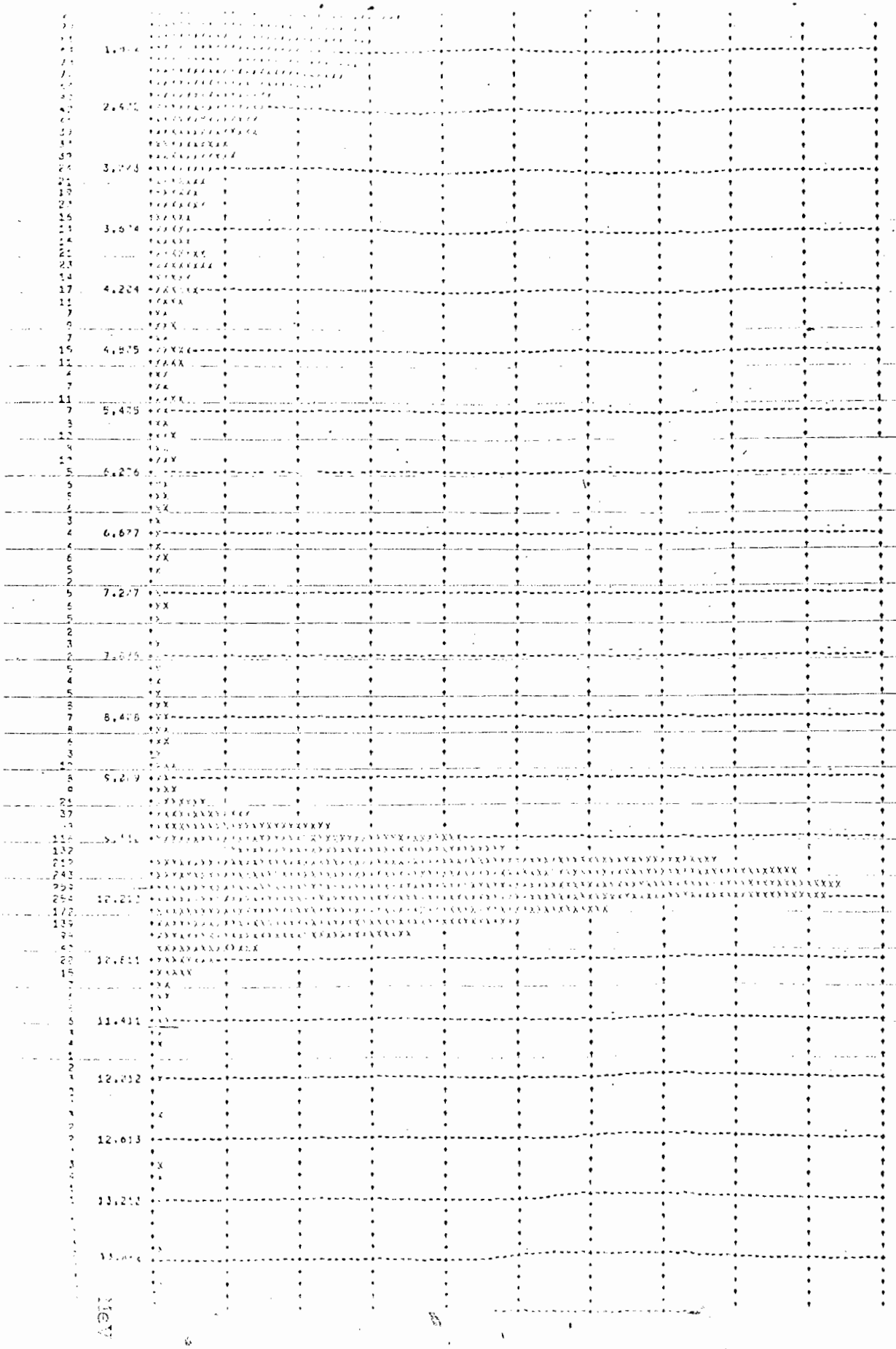

FIGURE 6

ON DMG

DET. NO.	REQ'D	FINISHED SIZE	MATERIAL

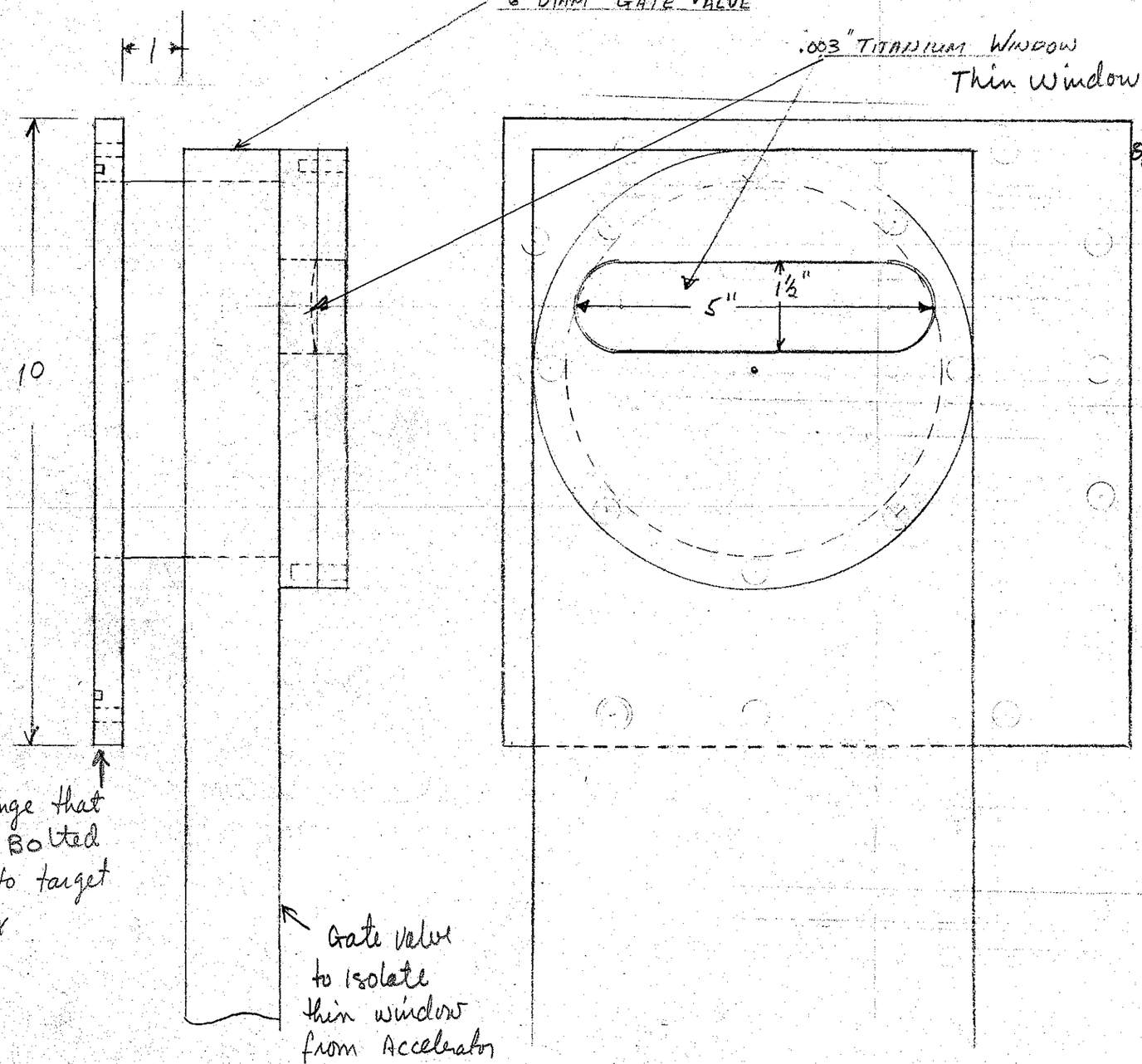

Thin window allowing recoil measurements from $\theta_L = 85°$ to $\theta_R = 50°$

NO.	REVISIONS	BY	DATE

130" CYCLOTRON LABORATORY
PHYSICS DEPT.
UNIVERSITY OF ROCHESTER

DWG. TITLE: PROPOSAL 198
THIN WINDOW FOR MAGNETIC SPECTROMETER

DR.	DATE:	FOR
C'K'D	DATE:	

REMOVE ALL BURRS & SHARP EDGES
TOLERANCES UNLESS OTHERWISE SPECIFIED
DECIMALS ± FRACTIONS ± ANGLES ±

SCALE	SHEET ____ OF ____ SHEETS	DWG. NO.
HALF		

DWG. NO.

DET. NO.	REQ'D	FINISHED SIZE	MATERIAL

OPENING FOR EXPERIMENT 36

BEAM

TV PORT →

EXISTING HOLE IN VACUUM BOX FOR EXPERIMENT 67/188

6"

8"

PROPOSED OPENING FOR PROPOSAL 198

BOTTOM PLATE OF BOX

NO.	REVISIONS	BY	DATE

130" CYCLOTRON LABORATORY
PHYSICS DEPT.
UNIVERSITY OF ROCHESTER

DWG. TITLE

PROPOSAL 198
MODIFICATION TO VACUUM BOX

DR.	DATE:	FOR
C'K'D	DATE:	

REMOVE ALL BURRS & SHARP EDGES
TOLERANCES UNLESS OTHERWISE SPECIFIED
DECIMALS ± FRACTIONS ± ANGLES ±

SCALE	SHEET ____ OF ____ SHEETS	DWG. NO.
HALF		

2/8/74

Up-date on Proposal 198 for Jet Target in Expanded C-O Area

The experimental set-up is shown in Figs. 1 and 2. The spectrometer consists of two quads and two bending magnets. We show standard ZGS magnets (specs. enclosed, Figs. 9, 10 and 11) but any similar or superconducting magnets would do. The magnets would be mounted on a rigid platform which pivots around the target so that the spectrometer could be remotely controlled to view recoils from 45° to 90° in the lab.

Quads

The main function of the quads is to focus parallel rays (rays having the same θ) to a point at the first wire chamber (see Fig. 3). Machine vacuum is extended up to this first wire plane (see Fig. 1). The recoil angle will thus be determined by measuring one point and will be independent of multiple scattering. The second function of the quads is to increase the solid angle, especially $\Delta\phi$ (Fig. 3).

Bending Magnets

The recoil momentum resolution is limited by multiple scattering in the middle wire plane (PC3 in Fig. 1) and helium. Multiple scattering in PC2 and PC4 does not contribute. To minimize the uncertainty in recoil momentum we bend by a large angle; 60° for recoil momenta up to $\sim$1 GeV/c. At higher momenta, given the same magnets, we bend less. We foresee perhaps two, at most three, different bend angles to cover the proposed range ($0.15 < |t| < 3.0$ GeV^2). Although we bend less at high $|t|$, the loss in resolution is partially compensated by the lower multiple scattering at high momenta.

Interface To Machine Vacuum

To get machine vacuum to PC1 and maintain freedom of motion we might use a 6" diameter foot long stainless steel bellows a foot to one and one half feet from the target. This would allow pivoting by $\pm 6^{\circ}$. Angles outside the range would be reached by "shimming" the front end of the bellows with wedge shaped 6" diameter washers

to give us different "central" angles. Four shims would be needed to cover $45^{\circ} < \theta < 90^{\circ}$. A gate valve between bellows and target would separate machine and spectrometer vacuum during angle changes.

Counting Rate

The large solid angle resulting from the quads would give an elastic counting rate of 10/machine pulse at 2.5×10^{12} protons/pulse in the region of the "dip" at $|t| \simeq 1.4$ GeV^2.

Monte Carlo Resolution Studies

The proposed apparatus has been "assembled" inside the memory of a PDP-10. We allow an elastic event to occur somewhere (randomly) in the beam-jet region and we follow the scattered proton through the apparatus, allowing it to randomly scatter wherever it meets an obstacle. When it passes a wire plane we make note of the nearest wire. From the struck wire in the first plane (made up of double planes with 1.5 mm wire spacing each to give an effective spacing of 0.75 mm) we infer the recoil angle. We "fit" a recoil momentum to the three struck wires in the last three planes (single planes, 1.5 mm wire spacing). From the θ_{recoil} and p_{recoil} so found we calculate a missing mass. The results are given in Figs. 4, 5 and 6. Chromatic aberrations due to $\Delta p_{recoil} = \pm 4\%$ have been included.

Our conservative estimates of the expected elastic mass resolution for the "real" spectrometer at 400 GeV incident energy are: $\Delta M = \pm 87$, ± 137 and ± 169 MeV at $|t| = 0.15$, 1.5 and 3.0 GeV^2 respectively. Mass resolutions at energies other than 400 GeV can be obtained by multiplying the above values by E/400, e.g., at 100 GeV and 1000 GeV they would be 0.25 and 2.5 times the above values respectively.

The resolution in momemtum transfer t at 400 GeV and $t = -1.5$ GeV^2 is $\Delta t = \pm 0.0012$ GeV^2 (See Fig. 7).

For heavy missing masses produced in inelastic collisions the resolution improves dramatically. For example, if the spectrometer is placed at the Jacobian peak, then $\partial M/\partial p_{recoil} = 0$,

$\partial M/\partial\theta_{recoil}$ is much less than for elastic and indeed the limiting factor is $\partial M/\partial p_{inc}$. At 400 GeV, $t = -0.5$ GeV^2 we get (from Monte Carlo) $\Delta M = \pm 10$ MeV for MM = 13.0 GeV (see Fig. 8).

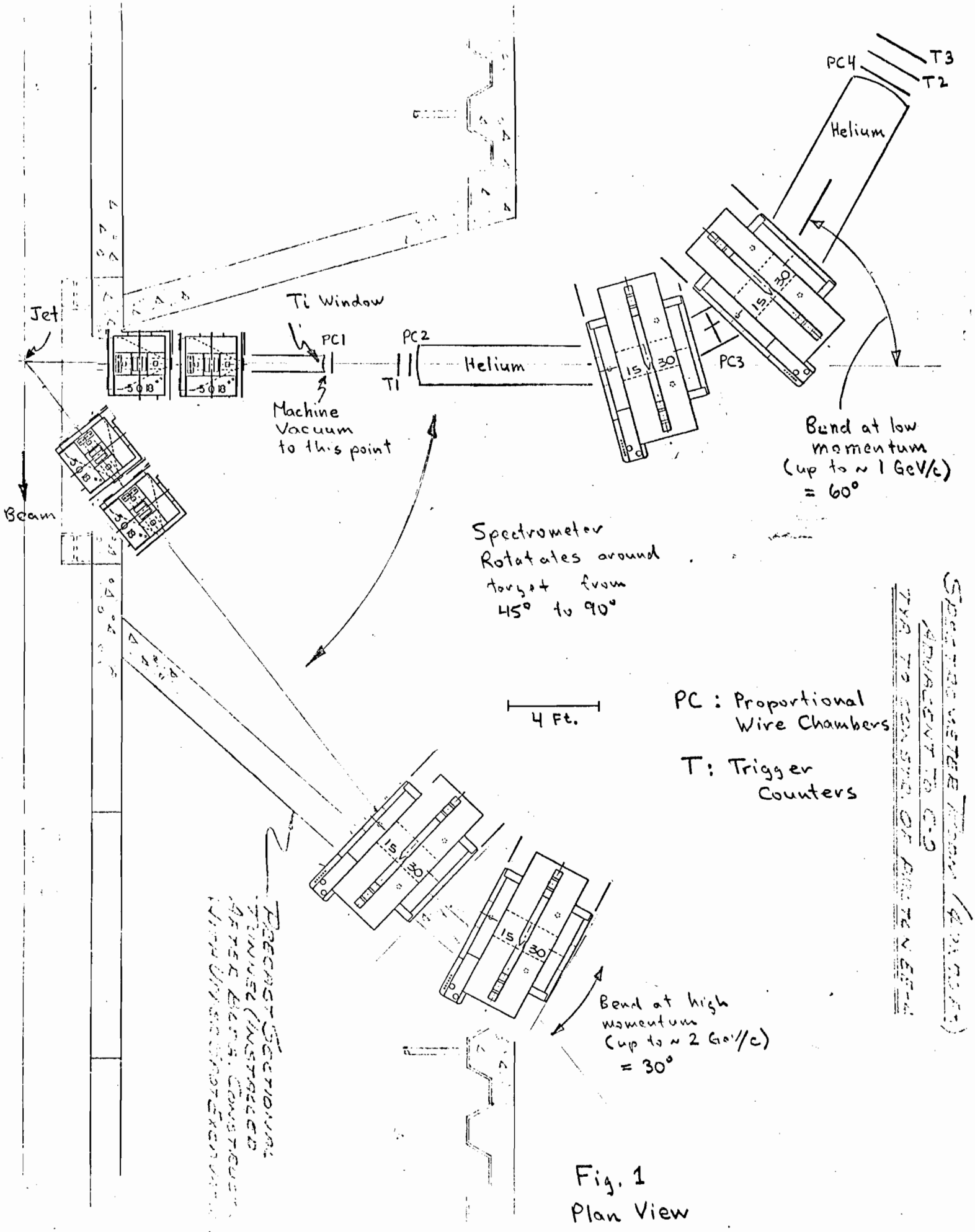

Fig. 1
Plan View

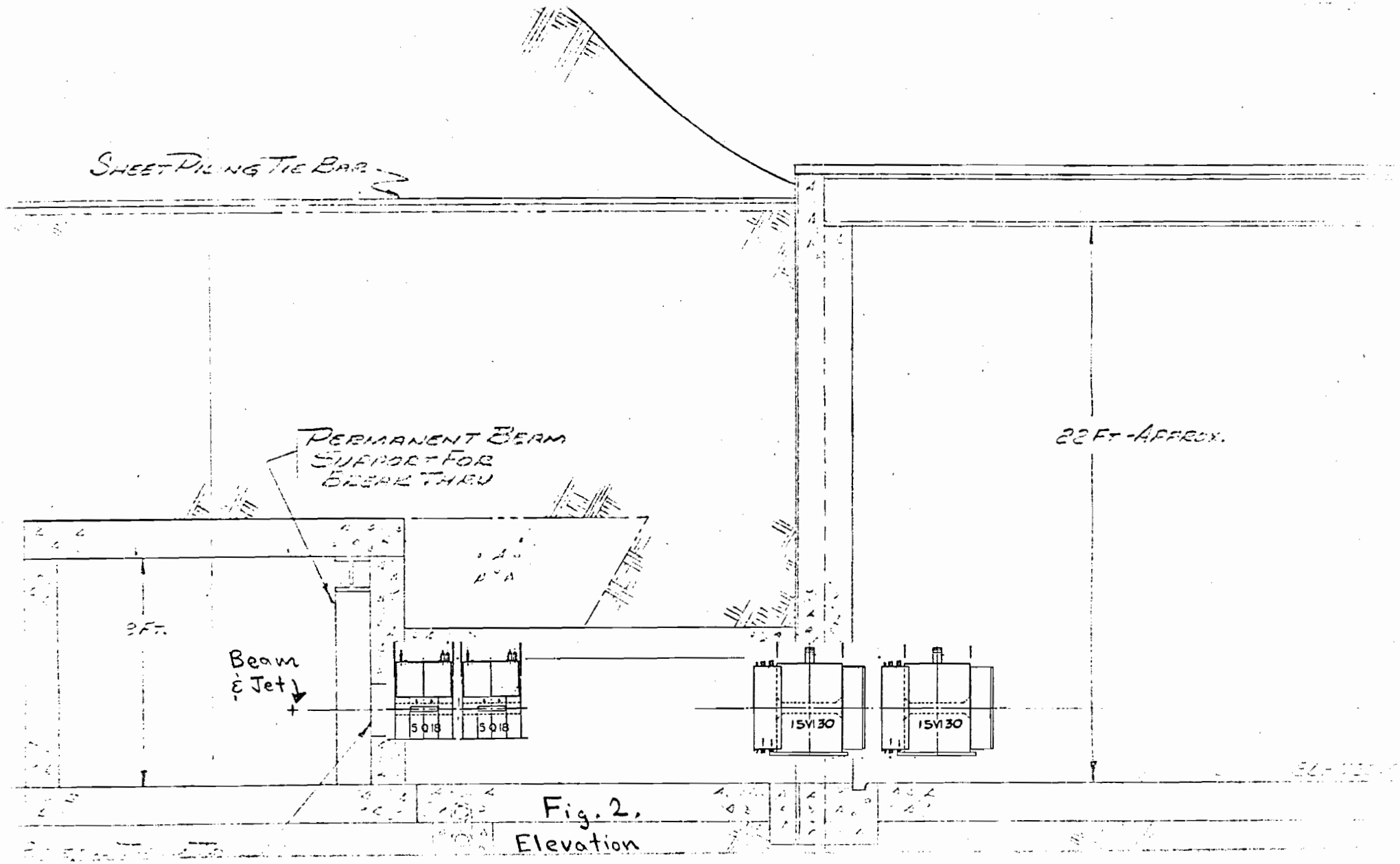

Fig. 2.
Elevation

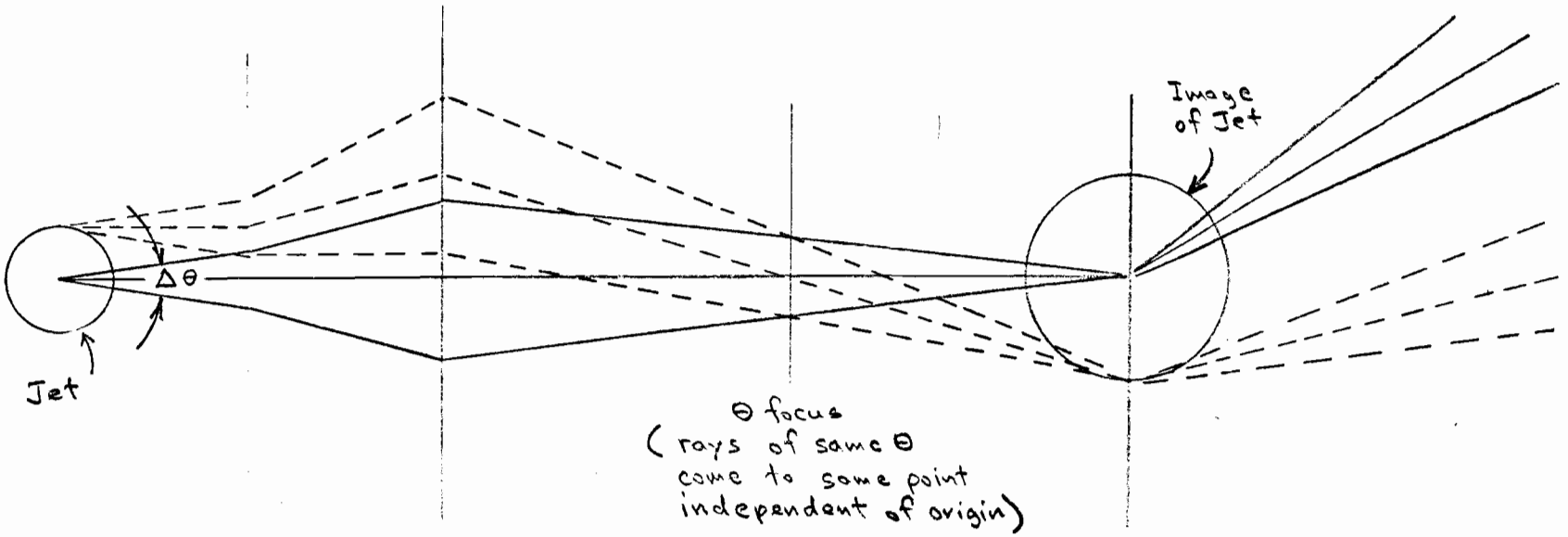

Fig. 3 Beam Optics
(Not to scale except for
relative beam, jet and image sizes)

HISTOGRAM NO. 1 SUM = 0.50000E+03 NORMALIZED TO 0.00000E+00 SCALE = 1.10
VAR.-TEST NO. 1- 0

$$$$$$$$$********* M4 *********$$$$$$$$$

Mass (GeV)

X .LT.	0.31428E+00	=	0.00000E+00	+-	0.00000E+00	I
0.31428E+00 .LE. X .LT.	0.33928E+00	=	0.00000E+00	+-	0.00000E+00	I
0.33928E+00 .LE. X .LT.	0.36428E+00	=	0.00000E+00	+-	0.00000E+00	I
0.36428E+00 .LE. X .LT.	0.38928E+00	=	0.00000E+00	+-	0.00000E+00	I
0.38928E+00 .LE. X .LT.	0.41428E+00	=	0.00000E+00	+-	0.00000E+00	I
0.41428E+00 .LE. X .LT.	0.43928E+00	=	0.00000E+00	+-	0.00000E+00	I
0.43928E+00 .LE. X .LT.	0.46428E+00	=	0.00000E+00	+-	0.00000E+00	I
0.46428E+00 .LE. X .LT.	0.48928E+00	=	0.00000E+00	+-	0.00000E+00	I
0.48928E+00 .LE. X .LT.	0.51428E+00	=	0.10000E+01	+-	0.10000E+01	I
0.51428E+00 .LE. X .LT.	0.53928E+00	=	0.00000E+00	+-	0.00000E+00	I
0.53928E+00 .LE. X .LT.	0.56428E+00	=	0.00000E+00	+-	0.00000E+00	I
0.56428E+00 .LE. X .LT.	0.58928E+00	=	0.00000E+00	+-	0.00000E+00	I
0.58928E+00 .LE. X .LT.	0.61428E+00	=	0.00000E+00	+-	0.00000E+00	I
0.61428E+00 .LE. X .LT.	0.63928E+00	=	0.00000E+00	+-	0.00000E+00	I
0.63928E+00 .LE. X .LT.	0.66428E+00	=	0.20000E+01	+-	0.14142E+01	I*
0.66428E+00 .LE. X .LT.	0.68928E+00	=	0.20000E+01	+-	0.14142E+01	I*
0.68928E+00 .LE. X .LT.	0.71428E+00	=	0.10000E+01	+-	0.10000E+01	I
0.71428E+00 .LE. X .LT.	0.73928E+00	=	0.20000E+01	+-	0.14142E+01	I*
0.73928E+00 .LE. X .LT.	0.76428E+00	=	0.80000E+01	+-	0.28284E+01	I*******
0.76428E+00 .LE. X .LT.	0.78928E+00	=	0.16000E+02	+-	0.40000E+01	I***************
0.78928E+00 .LE. X .LT.	0.81428E+00	=	0.20000E+02	+-	0.44721E+01	I*******************
0.81428E+00 .LE. X .LT.	0.83928E+00	=	0.24000E+02	+-	0.48990E+01	I************************
0.83928E+00 .LE. X .LT.	0.86428E+00	=	0.32000E+02	+-	0.56569E+01	I********************************
0.86428E+00 .LE. X .LT.	0.88928E+00	=	0.43000E+02	+-	0.65574E+01	I**
0.88928E+00 .LE. X .LT.	0.91428E+00	=	0.56000E+02	+-	0.74833E+01	I**
0.91428E+00 .LE. X .LT.	0.93928E+00	=	0.55000E+02	+-	0.74162E+01	I***
0.93928E+00 .LE. X .LT.	0.96428E+00	=	0.55000E+02	+-	0.74162E+01	I***
0.96428E+00 .LE. X .LT.	0.98928E+00	=	0.49000E+02	+-	0.70000E+01	I**
0.98928E+00 .LE. X .LT.	0.10143E+01	=	0.44000E+02	+-	0.66332E+01	I***
0.10143E+01 .LE. X .LT.	0.10393E+01	=	0.37000E+02	+-	0.60828E+01	I**********************************
0.10393E+01 .LE. X .LT.	0.10643E+01	=	0.26000E+02	+-	0.50990E+01	I************************
0.10643E+01 .LE. X .LT.	0.10893E+01	=	0.15000E+02	+-	0.38730E+01	I**************
0.10893E+01 .LE. X .LT.	0.11143E+01	=	0.60000E+01	+-	0.24495E+01	I*****
0.11143E+01 .LE. X .LT.	0.11393E+01	=	0.40000E+01	+-	0.20000E+01	I***
0.11393E+01 .LE. X .LT.	0.11643E+01	=	0.20000E+01	+-	0.14142E+01	I*
0.11643E+01 .LE. X .LT.	0.11893E+01	=	0.00000E+00	+-	0.00000E+00	I
0.11893E+01 .LE. X .LT.	0.12143E+01	=	0.00000E+00	+-	0.00000E+00	I
0.12143E+01 .LE. X .LT.	0.12393E+01	=	0.00000E+00	+-	0.00000E+00	I
0.12393E+01 .LE. X .LT.	0.12643E+01	=	0.00000E+00	+-	0.00000E+00	I
0.12643E+01 .LE. X .LT.	0.12893E+01	=	0.00000E+00	+-	0.00000E+00	I
0.12893E+01 .LE. X .LT.	0.13143E+01	=	0.00000E+00	+-	0.00000E+00	I
0.13143E+01 .LE. X .LT.	0.13393E+01	=	0.00000E+00	+-	0.00000E+00	I
0.13393E+01 .LE. X .LT.	0.13643E+01	=	0.00000E+00	+-	0.00000E+00	I
0.13643E+01 .LE. X .LT.	0.13893E+01	=	0.00000E+00	+-	0.00000E+00	I
0.13893E+01 .LE. X .LT.	0.14143E+01	=	0.00000E+00	+-	0.00000E+00	I
0.14143E+01 .LE. X .LT.	0.14393E+01	=	0.00000E+00	+-	0.00000E+00	I
0.14393E+01 .LE. X .LT.	0.14643E+01	=	0.00000E+00	+-	0.00000E+00	I
0.14643E+01 .LE. X .LT.	0.14893E+01	=	0.00000E+00	+-	0.00000E+00	I
0.14893E+01 .LE. X .LT.	0.15143E+01	=	0.00000E+00	+-	0.00000E+00	I
0.15143E+01 .LE. X .LT.	0.15393E+01	=	0.00000E+00	+-	0.00000E+00	I
0.15393E+01 .LE. X .LT.	0.15643E+01	=	0.00000E+00	+-	0.00000E+00	I
0.15643E+01 .LE. X		=	0.00000E+00	+-	0.00000E+00	I

N(938)

Mass (GeV)

N*(1236)

Fig 4
Mass resolution for elastic scattering at E = 400 GeV t = -0.15 GeV^2
Mass = ± 87 MeV.

HISTOGRAM NO. 1 SUM = 0.49800E+03 NORMALIZED TO 0.00000E+00 SCALE = 1.00
VAR.-TEST NO. 1- 0

$$$$$$$$$********* M4 *********$$$$$$$$$

Mass (GeV)

		X	.LT.	0.31206E+00	=	0.20000E+01	+-	0.14142E+01
0.31206E+00	.LE.	X	.LT.	0.33706E+00	=	0.00000E+00	+-	0.00000E+00
0.33706E+00	.LE.	X	.LT.	0.36206E+00	=	0.00000E+00	+-	0.00000E+00
0.36206E+00	.LE.	X	.LT.	0.38706E+00	=	0.00000E+00	+-	0.00000E+00
0.38706E+00	.LE.	X	.LT.	0.41206E+00	=	0.10000E+01	+-	0.10000E+01
0.41206E+00	.LE.	X	.LT.	0.43706E+00	=	0.10000E+01	+-	0.10000E+01
0.43706E+00	.LE.	X	.LT.	0.46206E+00	=	0.10000E+01	+-	0.10000E+01
0.46206E+00	.LE.	X	.LT.	0.48706E+00	=	0.00000E+00	+-	0.00000E+00
0.48706E+00	.LE.	X	.LT.	0.51206E+00	=	0.20000E+01	+-	0.14142E+01
0.51206E+00	.LE.	X	.LT.	0.53706E+00	=	0.20000E+01	+-	0.14142E+01
0.53706E+00	.LE.	X	.LT.	0.56206E+00	=	0.30000E+01	+-	0.17321E+01
0.56206E+00	.LE.	X	.LT.	0.58706E+00	=	0.80000E+01	+-	0.28284E+01
0.58706E+00	.LE.	X	.LT.	0.61206E+00	=	0.40000E+01	+-	0.20000E+01
0.61206E+00	.LE.	X	.LT.	0.63706E+00	=	0.30000E+01	+-	0.17321E+01
0.63706E+00	.LE.	X	.LT.	0.66206E+00	=	0.90000E+01	+-	0.30000E+01
0.66206E+00	.LE.	X	.LT.	0.68706E+00	=	0.80000E+01	+-	0.28284E+01
0.68706E+00	.LE.	X	.LT.	0.71206E+00	=	0.80000E+01	+-	0.28284E+01
0.71206E+00	.LE.	X	.LT.	0.73706E+00	=	0.14000E+02	+-	0.37417E+01
0.73706E+00	.LE.	X	.LT.	0.76206E+00	=	0.21000E+02	+-	0.45826E+01
0.76206E+00	.LE.	X	.LT.	0.78706E+00	=	0.23000E+02	+-	0.47958E+01
0.78706E+00	.LE.	X	.LT.	0.81206E+00	=	0.29000E+02	+-	0.53852E+01
0.81206E+00	.LE.	X	.LT.	0.83706E+00	=	0.26000E+02	+-	0.50990E+01
0.83706E+00	.LE.	X	.LT.	0.86206E+00	=	0.45000E+02	+-	0.67082E+01
0.86206E+00	.LE.	X	.LT.	0.88706E+00	=	0.30000E+02	+-	0.54772E+01
0.88706E+00	.LE.	X	.LT.	0.91206E+00	=	0.42000E+02	+-	0.64807E+01
0.91206E+00	.LE.	X	.LT.	0.93706E+00	=	0.29000E+02	+-	0.53852E+01
0.93706E+00	.LE.	X	.LT.	0.96206E+00	=	0.34000E+02	+-	0.58310E+01
0.96206E+00	.LE.	X	.LT.	0.98706E+00	=	0.37000E+02	+-	0.60828E+01
0.98706E+00	.LE.	X	.LT.	0.10121E+01	=	0.24000E+02	+-	0.48990E+01
0.10121E+01	.LE.	X	.LT.	0.10371E+01	=	0.21000E+02	+-	0.45826E+01
0.10371E+01	.LE.	X	.LT.	0.10621E+01	=	0.22000E+02	+-	0.46904E+01
0.10621E+01	.LE.	X	.LT.	0.10871E+01	=	0.17000E+02	+-	0.41231E+01
0.10871E+01	.LE.	X	.LT.	0.11121E+01	=	0.16000E+02	+-	0.40000E+01
0.11121E+01	.LE.	X	.LT.	0.11371E+01	=	0.90000E+01	+-	0.30000E+01
0.11371E+01	.LE.	X	.LT.	0.11621E+01	=	0.60000E+01	+-	0.24495E+01
0.11621E+01	.LE.	X	.LT.	0.11871E+01	=	0.00000E+00	+-	0.00000E+00
0.11871E+01	.LE.	X	.LT.	0.12121E+01	=	0.10000E+01	+-	0.10000E+01
0.12121E+01	.LE.	X	.LT.	0.12371E+01	=	0.10000E+01	+-	0.10000E+01
0.12371E+01	.LE.	X	.LT.	0.12621E+01	=	0.10000E+01	+-	0.10000E+01
0.12621E+01	.LE.	X	.LT.	0.12871E+01	=	0.00000E+00	+-	0.00000E+00
0.12871E+01	.LE.	X	.LT.	0.13121E+01	=	0.00000E+00	+-	0.00000E+00
0.13121E+01	.LE.	X	.LT.	0.13371E+01	=	0.00000E+00	+-	0.00000E+00
0.13371E+01	.LE.	X	.LT.	0.13621E+01	=	0.00000E+00	+-	0.00000E+00
0.13621E+01	.LE.	X	.LT.	0.13871E+01	=	0.00000E+00	+-	0.00000E+00
0.13871E+01	.LE.	X	.LT.	0.14121E+01	=	0.00000E+00	+-	0.00000E+00
0.14121E+01	.LE.	X	.LT.	0.14371E+01	=	0.00000E+00	+-	0.00000E+00
0.14371E+01	.LE.	X	.LT.	0.14621E+01	=	0.00000E+00	+-	0.00000E+00
0.14621E+01	.LE.	X	.LT.	0.14871E+01	=	0.00000E+00	+-	0.00000E+00
0.14871E+01	.LE.	X	.LT.	0.15121E+01	=	0.00000E+00	+-	0.00000E+00
0.15121E+01	.LE.	X	.LT.	0.15371E+01	=	0.00000E+00	+-	0.00000E+00
0.15371E+01	.LE.	X	.LT.	0.15621E+01	=	0.00000E+00	+-	0.00000E+00
0.15621E+01	.LE.	X			=	0.00000E+00	+-	0.00000E+00

N(938)

N*(1236)

Mass (GeV)

Mass resolution = ± 137 MeV

Fig. 5

Mass resolution for elastic scattering at E = 400 GeV t = -1.5 GeV²

HISTOGRAM NO. 1 SUM = 0.49500E+03 NORMALIZED TO 0.00000E+00 SCALE = 1.00
VAR.-TEST NO. 1- 0

$$$$$$$$$*********** M4 **********$$$$$$$$$

Mass (GeV)

	X .LT.	0.31205E+00	=	0.50000E+01	+-	0.22361E+01	I*****
0.31205E+00	.LE. X .LT.	0.33705E+00	=	0.20000E+01	+-	0.14142E+01	I**
0.33705E+00	.LE. X .LT.	0.36205E+00	=	0.00000E+00	+-	0.00000E+00	I
0.36205E+00	.LE. X .LT.	0.38705E+00	=	0.00000E+00	+-	0.00000E+00	I
0.38705E+00	.LE. X .LT.	0.41205E+00	=	0.20000E+01	+-	0.14142E+01	I**
0.41205E+00	.LE. X .LT.	0.43705E+00	=	0.00000E+00	+-	0.00000E+00	I
0.43705E+00	.LE. X .LT.	0.46205E+00	=	0.40000E+01	+-	0.20000E+01	I****
0.46205E+00	.LE. X .LT.	0.48705E+00	=	0.60000E+01	+-	0.24495E+01	I******
0.48705E+00	.LE. X .LT.	0.51205E+00	=	0.30000E+01	+-	0.17321E+01	I***
0.51205E+00	.LE. X .LT.	0.53705E+00	=	0.40000E+01	+-	0.20000E+01	I****
0.53705E+00	.LE. X .LT.	0.56205E+00	=	0.80000E+01	+-	0.28284E+01	I********
0.56205E+00	.LE. X .LT.	0.58705E+00	=	0.13000E+02	+-	0.36056E+01	I*************
0.58705E+00	.LE. X .LT.	0.61205E+00	=	0.80000E+01	+-	0.28284E+01	I********
0.61205E+00	.LE. X .LT.	0.63705E+00	=	0.70000E+01	+-	0.26458E+01	I*******
0.63705E+00	.LE. X .LT.	0.66205E+00	=	0.80000E+01	+-	0.28284E+01	I********
0.66205E+00	.LE. X .LT.	0.68705E+00	=	0.19000E+02	+-	0.43589E+01	I*******************
0.68705E+00	.LE. X .LT.	0.71205E+00	=	0.25000E+02	+-	0.50000E+01	I*************************
0.71205E+00	.LE. X .LT.	0.73705E+00	=	0.15000E+02	+-	0.38730E+01	I***************
0.73705E+00	.LE. X .LT.	0.76205E+00	=	0.12000E+02	+-	0.34641E+01	I************
0.76205E+00	.LE. X .LT.	0.78705E+00	=	0.17000E+02	+-	0.41231E+01	I*****************
0.78705E+00	.LE. X .LT.	0.81205E+00	=	0.30000E+02	+-	0.54772E+01	I******************************
0.81205E+00	.LE. X .LT.	0.83705E+00	=	0.21000E+02	+-	0.45826E+01	I*********************
0.83705E+00	.LE. X .LT.	0.86205E+00	=	0.29000E+02	+-	0.53852E+01	I*****************************
0.86205E+00	.LE. X .LT.	0.88705E+00	=	0.35000E+02	+-	0.59161E+01	I**********************************
0.88705E+00	.LE. X .LT.	0.91205E+00	=	0.38000E+02	+-	0.61644E+01	I*************************************
0.91205E+00	.LE. X .LT.	0.93705E+00	=	0.32000E+02	+-	0.56569E+01	I********************************
0.93705E+00	.LE. X .LT.	0.96205E+00	=	0.27000E+02	+-	0.51962E+01	I***************************
0.96205E+00	.LE. X .LT.	0.98705E+00	=	0.31000E+02	+-	0.55678E+01	I*******************************
0.98705E+00	.LE. X .LT.	0.10121E+01	=	0.23000E+02	+-	0.47958E+01	I***********************
0.10121E+01	.LE. X .LT.	0.10371E+01	=	0.12000E+02	+-	0.34641E+01	I************
0.10371E+01	.LE. X .LT.	0.10621E+01	=	0.11000E+02	+-	0.33166E+01	I***********
0.10621E+01	.LE. X .LT.	0.10871E+01	=	0.13000E+02	+-	0.36056E+01	I*************
0.10871E+01	.LE. X .LT.	0.11121E+01	=	0.14000E+02	+-	0.37417E+01	I**************
0.11121E+01	.LE. X .LT.	0.11371E+01	=	0.60000E+01	+-	0.24495E+01	I******
0.11371E+01	.LE. X .LT.	0.11621E+01	=	0.90000E+01	+-	0.30000E+01	I*********
0.11621E+01	.LE. X .LT.	0.11871E+01	=	0.40000E+01	+-	0.20000E+01	I****
0.11871E+01	.LE. X .LT.	0.12121E+01	=	0.30000E+01	+-	0.17321E+01	I***
0.12121E+01	.LE. X .LT.	0.12371E+01	=	0.10000E+01	+-	0.10000E+01	I*
0.12371E+01	.LE. X .LT.	0.12621E+01	=	0.20000E+01	+-	0.14142E+01	I**
0.12621E+01	.LE. X .LT.	0.12871E+01	=	0.10000E+01	+-	0.10000E+01	I*
0.12871E+01	.LE. X .LT.	0.13121E+01	=	0.00000E+00	+-	0.00000E+00	I
0.13121E+01	.LE. X .LT.	0.13371E+01	=	0.00000E+00	+-	0.00000E+00	I
0.13371E+01	.LE. X .LT.	0.13621E+01	=	0.00000E+00	+-	0.00000E+00	I
0.13621E+01	.LE. X .LT.	0.13871E+01	=	0.00000E+00	+-	0.00000E+00	I
0.13871E+01	.LE. X .LT.	0.14121E+01	=	0.00000E+00	+-	0.00000E+00	I
0.14121E+01	.LE. X .LT.	0.14371E+01	=	0.00000E+00	+-	0.00000E+00	I
0.14371E+01	.LE. X .LT.	0.14621E+01	=	0.00000E+00	+-	0.00000E+00	I
0.14621E+01	.LE. X .LT.	0.14871E+01	=	0.00000E+00	+-	0.00000E+00	I
0.14871E+01	.LE. X .LT.	0.15121E+01	=	0.00000E+00	+-	0.00000E+00	I
0.15121E+01	.LE. X .LT.	0.15371E+01	=	0.00000E+00	+-	0.00000E+00	I
0.15371E+01	.LE. X .LT.	0.15621E+01	=	0.00000E+00	+-	0.00000E+00	I
0.15621E+01	.LE. X		=	0.00000E+00	+-	0.00000E+00	I

N(938)

Mass (GeV)

N*(1236)

N*(1520)

$q_{Mass} = \pm 169$ MeV

Fig. 6
Mass resolution for Elastic scattering at E = 400 GeV
t = - 3.0 GeV^2

HISTOGRAM NO. 3 SUM = 0.50000E+03 NORMALIZED TO 0.00000E+00 SCALE = 3.59
VAR.-TEST NO. 2- 0

$$$$$$$$$********* T *********$$$$$$$$$

t (GeV²)

X .LT. -0.15844E+01	=	0.00000E+00	+-	0.00000E+00	I
-0.15844E+01 .LE. X .LT. -0.15834E+01	=	0.00000E+00	+-	0.00000E+00	I
-0.15834E+01 .LE. X .LT. -0.15824E+01	=	0.00000E+00	+-	0.00000E+00	I
-0.15824E+01 .LE. X .LT. -0.15814E+01	=	0.00000E+00	+-	0.00000E+00	I
-0.15814E+01 .LE. X .LT. -0.15804E+01	=	0.00000E+00	+-	0.00000E+00	I
-0.15804E+01 .LE. X .LT. -0.15794E+01	=	0.00000E+00	+-	0.00000E+00	I
-0.15794E+01 .LE. X .LT. -0.15784E+01	=	0.00000E+00	+-	0.00000E+00	I
-0.15784E+01 .LE. X .LT. -0.15774E+01	=	0.00000E+00	+-	0.00000E+00	I
-0.15774E+01 .LE. X .LT. -0.15764E+01	=	0.00000E+00	+-	0.00000E+00	I
-0.15764E+01 .LE. X .LT. -0.15754E+01	=	0.00000E+00	+-	0.00000E+00	I
-0.15754E+01 .LE. X .LT. -0.15744E+01	=	0.00000E+00	+-	0.00000E+00	I
-0.15744E+01 .LE. X .LT. -0.15734E+01	=	0.00000E+00	+-	0.00000E+00	I
-0.15734E+01 .LE. X .LT. -0.15724E+01	=	0.00000E+00	+-	0.00000E+00	I
-0.15724E+01 .LE. X .LT. -0.15714E+01	=	0.00000E+00	+-	0.00000E+00	I
-0.15714E+01 .LE. X .LT. -0.15704E+01	=	0.00000E+00	+-	0.00000E+00	I
-0.15704E+01 .LE. X .LT. -0.15694E+01	=	0.00000E+00	+-	0.00000E+00	I
-0.15694E+01 .LE. X .LT. -0.15684E+01	=	0.00000E+00	+-	0.00000E+00	I
-0.15684E+01 .LE. X .LT. -0.15674E+01	=	0.00000E+00	+-	0.00000E+00	I
-0.15674E+01 .LE. X .LT. -0.15664E+01	=	0.00000E+00	+-	0.00000E+00	I
-0.15664E+01 .LE. X .LT. -0.15654E+01	=	0.00000E+00	+-	0.00000E+00	I
-0.15654E+01 .LE. X .LT. -0.15644E+01	=	0.00000E+00	+-	0.00000E+00	I
-0.15644E+01 .LE. X .LT. -0.15634E+01	=	0.00000E+00	+-	0.00000E+00	I
-0.15634E+01 .LE. X .LT. -0.15624E+01	=	0.10000E+02	+-	0.31623E+01	I**
-0.15624E+01 .LE. X .LT. -0.15614E+01	=	0.33000E+02	+-	0.57446E+01	I*********
-0.15614E+01 .LE. X .LT. -0.15604E+01	=	0.12400E+03	+-	0.11136E+02	I**********************************
-0.15604E+01 .LE. X .LT. -0.15594E+01	=	0.18300E+03	+-	0.13528E+02	I**
-0.15594E+01 .LE. X .LT. -0.15584E+01	=	0.10900E+03	+-	0.10440E+02	I*****************************
-0.15584E+01 .LE. X .LT. -0.15574E+01	=	0.37000E+02	+-	0.60828E+01	I**********
-0.15574E+01 .LE. X .LT. -0.15564E+01	=	0.40000E+01	+-	0.20000E+01	I*
-0.15564E+01 .LE. X .LT. -0.15554E+01	=	0.00000E+00	+-	0.00000E+00	I
-0.15554E+01 .LE. X .LT. -0.15544E+01	=	0.00000E+00	+-	0.00000E+00	I
-0.15544E+01 .LE. X .LT. -0.15534E+01	=	0.00000E+00	+-	0.00000E+00	I
-0.15534E+01 .LE. X .LT. -0.15524E+01	=	0.00000E+00	+-	0.00000E+00	I
-0.15524E+01 .LE. X .LT. -0.15514E+01	=	0.00000E+00	+-	0.00000E+00	I
-0.15514E+01 .LE. X .LT. -0.15504E+01	=	0.00000E+00	+-	0.00000E+00	I
-0.15504E+01 .LE. X .LT. -0.15494E+01	=	0.00000E+00	+-	0.00000E+00	I
-0.15494E+01 .LE. X .LT. -0.15484E+01	=	0.00000E+00	+-	0.00000E+00	I
-0.15484E+01 .LE. X .LT. -0.15474E+01	=	0.00000E+00	+-	0.00000E+00	I
-0.15474E+01 .LE. X .LT. -0.15464E+01	=	0.00000E+00	+-	0.00000E+00	I
-0.15464E+01 .LE. X .LT. -0.15454E+01	=	0.00000E+00	+-	0.00000E+00	I
-0.15454E+01 .LE. X .LT. -0.15444E+01	=	0.00000E+00	+-	0.00000E+00	I
-0.15444E+01 .LE. X .LT. -0.15434E+01	=	0.00000E+00	+-	0.00000E+00	I
-0.15434E+01 .LE. X .LT. -0.15424E+01	=	0.00000E+00	+-	0.00000E+00	I
-0.15424E+01 .LE. X .LT. -0.15414E+01	=	0.00000E+00	+-	0.00000E+00	I
-0.15414E+01 .LE. X .LT. -0.15404E+01	=	0.00000E+00	+-	0.00000E+00	I
-0.15404E+01 .LE. X .LT. -0.15394E+01	=	0.00000E+00	+-	0.00000E+00	I
-0.15394E+01 .LE. X .LT. -0.15384E+01	=	0.00000E+00	+-	0.00000E+00	I
-0.15384E+01 .LE. X .LT. -0.15374E+01	=	0.00000E+00	+-	0.00000E+00	I
-0.15374E+01 .LE. X .LT. -0.15364E+01	=	0.00000E+00	+-	0.00000E+00	I
-0.15364E+01 .LE. X .LT. -0.15354E+01	=	0.00000E+00	+-	0.00000E+00	I
-0.15354E+01 .LE. X .LT. -0.15344E+01	=	0.00000E+00	+-	0.00000E+00	I
-0.15344E+01 .LE. X	=	0.00000E+00	+-	0.00000E+00	I

t (GeV²)

$\sigma_{|t|} = \pm 0.0012$ GeV²

Fig. 7
|t| resolution for Elastic Scattering at E = 400 GeV, t = -1.5 GeV²

HISTOGRAM NO. 1 SUM = 0.50000E+03 NORMALIZED TO 0.00000E+00 SCALE = 4.92
VAR.-TEST NO. 1- 0

$$$$$$$$$********** M4 **********$$$$$$$$$

Mass (GeV)

		X	.LT.	0.12377E+02	=	0.00000E+00	+-	0.00000E+00
0.12377E+02	.LE.	X	.LT.	0.12402E+02	=	0.00000E+00	+-	0.00000E+00
0.12402E+02	.LE.	X	.LT.	0.12427E+02	=	0.00000E+00	+-	0.00000E+00
0.12427E+02	.LE.	X	.LT.	0.12452E+02	=	0.00000E+00	+-	0.00000E+00
0.12452E+02	.LE.	X	.LT.	0.12477E+02	=	0.00000E+00	+-	0.00000E+00
0.12477E+02	.LE.	X	.LT.	0.12502E+02	=	0.00000E+00	+-	0.00000E+00
0.12502E+02	.LE.	X	.LT.	0.12527E+02	=	0.00000E+00	+-	0.00000E+00
0.12527E+02	.LE.	X	.LT.	0.12552E+02	=	0.00000E+00	+-	0.00000E+00
0.12552E+02	.LE.	X	.LT.	0.12577E+02	=	0.00000E+00	+-	0.00000E+00
0.12577E+02	.LE.	X	.LT.	0.12602E+02	=	0.00000E+00	+-	0.00000E+00
0.12602E+02	.LE.	X	.LT.	0.12627E+02	=	0.00000E+00	+-	0.00000E+00
0.12627E+02	.LE.	X	.LT.	0.12652E+02	=	0.00000E+00	+-	0.00000E+00
0.12652E+02	.LE.	X	.LT.	0.12677E+02	=	0.00000E+00	+-	0.00000E+00
0.12677E+02	.LE.	X	.LT.	0.12702E+02	=	0.00000E+00	+-	0.00000E+00
0.12702E+02	.LE.	X	.LT.	0.12727E+02	=	0.00000E+00	+-	0.00000E+00
0.12727E+02	.LE.	X	.LT.	0.12752E+02	=	0.00000E+00	+-	0.00000E+00
0.12752E+02	.LE.	X	.LT.	0.12777E+02	=	0.00000E+00	+-	0.00000E+00
0.12777E+02	.LE.	X	.LT.	0.12802E+02	=	0.00000E+00	+-	0.00000E+00
0.12802E+02	.LE.	X	.LT.	0.12827E+02	=	0.00000E+00	+-	0.00000E+00
0.12827E+02	.LE.	X	.LT.	0.12852E+02	=	0.00000E+00	+-	0.00000E+00
0.12852E+02	.LE.	X	.LT.	0.12877E+02	=	0.00000E+00	+-	0.00000E+00
0.12877E+02	.LE.	X	.LT.	0.12902E+02	=	0.00000E+00	+-	0.00000E+00
0.12902E+02	.LE.	X	.LT.	0.12927E+02	=	0.00000E+00	+-	0.00000E+00
0.12927E+02	.LE.	X	.LT.	0.12952E+02	=	0.00000E+00	+-	0.00000E+00
0.12952E+02	.LE.	X	.LT.	0.12977E+02	=	0.40000E+01	+-	0.20000E+01
0.12977E+02	.LE.	X	.LT.	0.13002E+02	=	0.24200E+03	+-	0.15556E+02
0.13002E+02	.LE.	X	.LT.	0.13027E+02	=	0.25100E+03	+-	0.15843E+02
0.13027E+02	.LE.	X	.LT.	0.13052E+02	=	0.30000E+01	+-	0.17321E+01
0.13052E+02	.LE.	X	.LT.	0.13077E+02	=	0.00000E+00	+-	0.00000E+00
0.13077E+02	.LE.	X	.LT.	0.13102E+02	=	0.00000E+00	+-	0.00000E+00
0.13102E+02	.LE.	X	.LT.	0.13127E+02	=	0.00000E+00	+-	0.00000E+00
0.13127E+02	.LE.	X	.LT.	0.13152E+02	=	0.00000E+00	+-	0.00000E+00
0.13152E+02	.LE.	X	.LT.	0.13177E+02	=	0.00000E+00	+-	0.00000E+00
0.13177E+02	.LE.	X	.LT.	0.13202E+02	=	0.00000E+00	+-	0.00000E+00
0.13202E+02	.LE.	X	.LT.	0.13227E+02	=	0.00000E+00	+-	0.00000E+00
0.13227E+02	.LE.	X	.LT.	0.13252E+02	=	0.00000E+00	+-	0.00000E+00
0.13252E+02	.LE.	X	.LT.	0.13277E+02	=	0.00000E+00	+-	0.00000E+00
0.13277E+02	.LE.	X	.LT.	0.13302E+02	=	0.00000E+00	+-	0.00000E+00
0.13302E+02	.LE.	X	.LT.	0.13327E+02	=	0.00000E+00	+-	0.00000E+00
0.13327E+02	.LE.	X	.LT.	0.13352E+02	=	0.00000E+00	+-	0.00000E+00
0.13352E+02	.LE.	X	.LT.	0.13377E+02	=	0.00000E+00	+-	0.00000E+00
0.13377E+02	.LE.	X	.LT.	0.13402E+02	=	0.00000E+00	+-	0.00000E+00
0.13402E+02	.LE.	X	.LT.	0.13427E+02	=	0.00000E+00	+-	0.00000E+00
0.13427E+02	.LE.	X	.LT.	0.13452E+02	=	0.00000E+00	+-	0.00000E+00
0.13452E+02	.LE.	X	.LT.	0.13477E+02	=	0.00000E+00	+-	0.00000E+00
0.13477E+02	.LE.	X	.LT.	0.13502E+02	=	0.00000E+00	+-	0.00000E+00
0.13502E+02	.LE.	X	.LT.	0.13527E+02	=	0.00000E+00	+-	0.00000E+00
0.13527E+02	.LE.	X	.LT.	0.13552E+02	=	0.00000E+00	+-	0.00000E+00
0.13552E+02	.LE.	X	.LT.	0.13577E+02	=	0.00000E+00	+-	0.00000E+00
0.13577E+02	.LE.	X	.LT.	0.13602E+02	=	0.00000E+00	+-	0.00000E+00
0.13602E+02	.LE.	X	.LT.	0.13627E+02	=	0.00000E+00	+-	0.00000E+00
0.13627E+02	.LE.	X			=	0.00000E+00	+-	0.00000E+00

MH = 13 GeV

Fig. 8 Mass resolution for Inelastic Scattering at Jacobian peak at E = 100 GeV t = -0.5 GeV/2 MH = 13.0 GeV

$q_{Mass} = \pm 10$ MeV

Mass (GeV)

15 VI 30 (BM 107) BENDING MAGNET

Measured Data - Central Field vs Magnet Current - Bending Angle vs Momentum

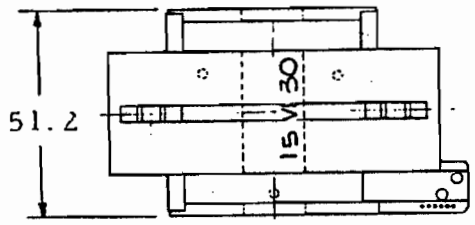

TOP VIEW

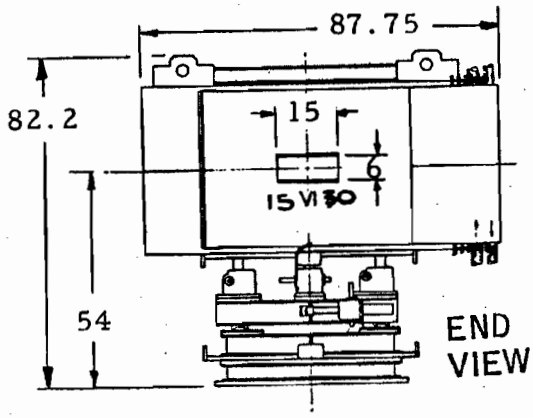

END VIEW

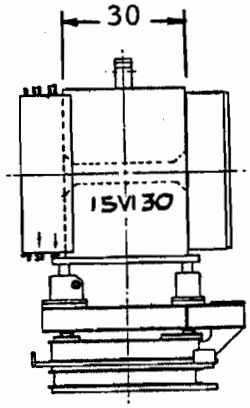

SIDE VIEW

Central Field vs Magnet Current

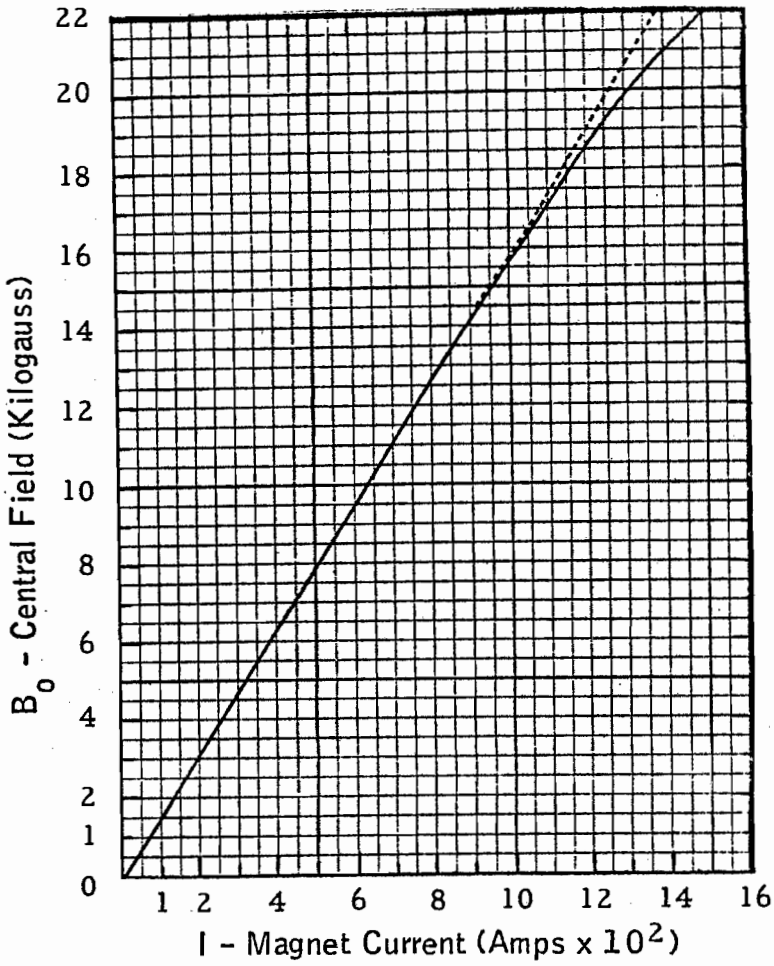

θ-P Curve

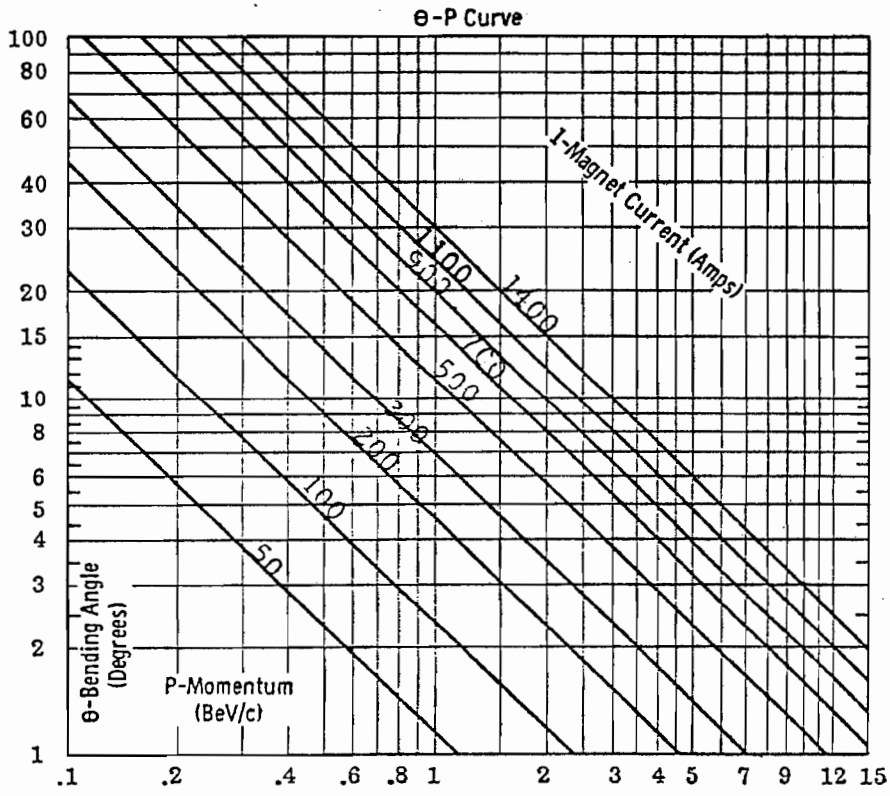

Total Weight:	18 Tons
Measured Data:	
Voltage	91 Volts dc
Current	1200 Amps dc
Power	109 kW
Field Strength	18.6 kG
Cooling Water (System Pressure Drop 200 psi)	
No. of Circuits	16
Pressure Drop	153 psi
Flow	14 gpm
Temp. Rise	54° F

Fig. 9

Percent Change of $\int Bd\ell$ Across the Gap - Mid Plane

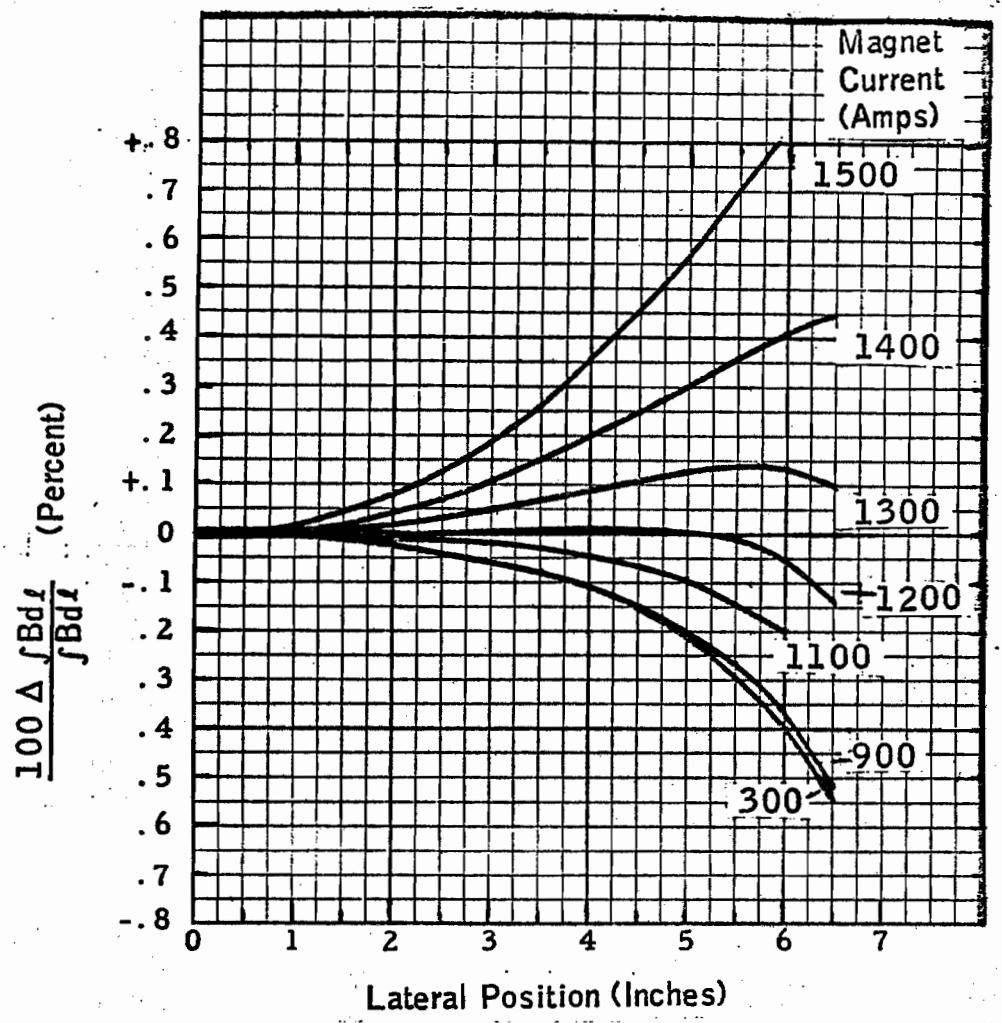

MAGNET		$\int Bd\ell$ (10^5 Gauss-In)	$\ell_o = \frac{\int Bd\ell}{B_o}$ Eff Length (Inches)±0.1	Central Field (Gauss)	
Current (Amps)	Terminal Voltage (Volts)			Up	Down
300	21	1.553	32.7	4741	4743
500	36	2.595	32.8	7898	7900
700	51	3.598	32.5	11050	11054
900	66	4.640	32.6	14189	14197
1100	82	5.613	32.5	17222	17237
1200	91	6.036	32.4	18614	18638
1300	99	6.452	32.4	19906	19929
1400	107	6.742	32.0	21054	21068
1500	116	6.972	31.8	21939	-

5.6 B

Fig. 10

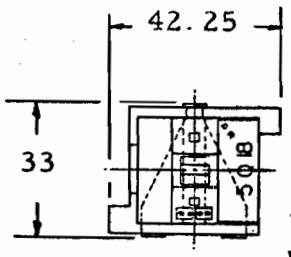

TOP VIEW

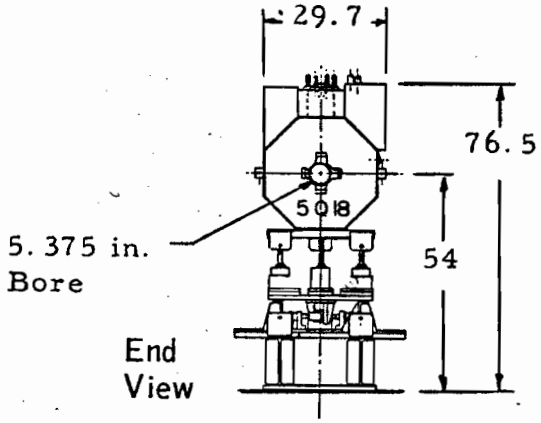

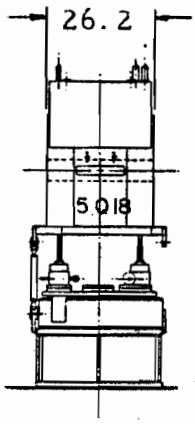

SIDE VIEW

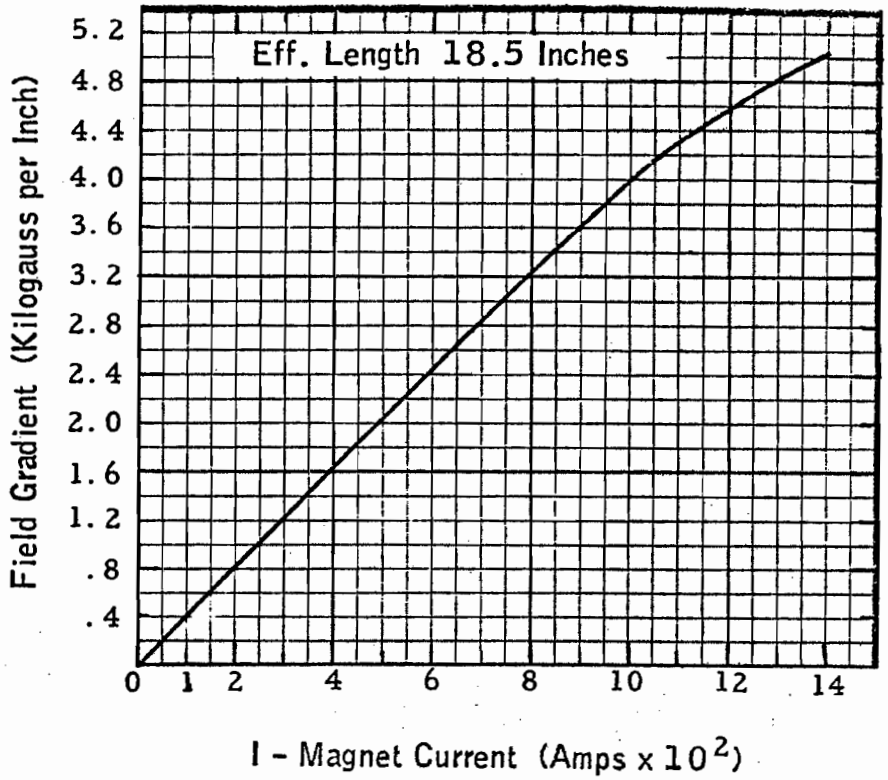

Total Weight:	2.0 Tons

Measured Data:

Voltage	77 Volts dc
Current	1200 Amps dc
Power	92 kW
Field Strength	13 kG

Cooling Water
(System Pressure Drop 200 psi)

No. of Circuits	12
Pressure Drop	127 psi
Flow	9 gpm
Temp. Rise	72° F

Current (Amps)	Terminal Voltage (Volts)	Gauss/ Inch
200	12	830
400	24	1644
600	36	2462
800	48	3266
1000	63	3985
1200	77	4574
1300	83	4833
1400	91	5054
Errors	± 2%	±0.5%

Fig. 11

Addendum to Proposal 198-A

A Proposal for a Magnetic Recoil Spectrometer for the Gas Jet Target

D. A. Gross, M. Miller, D. Nitz and S. L. Olsen
The University of Rochester, Rochester, N. Y. 14527

K. Abe, J. Alspector, K. Cohen, J. Mueller, B. Robinson and F. Sannes
Rutgers University, New Brunswick, N. J. 08903

D. A. Garbutt, R. Sarma and I. Siotis
Imperial College, London SW7, U. K.

ABSTRACT

We propose to measure recoils from the internal H_2 and D_2 gas jet target at incident energies up to 500 GeV and values of $|t|$ up to 5 GeV^2 using a single arm magnetic spectrometer. The wide range of incident energies, low target density and high luminosity available at the internal target are well suited for a high-resolution, high-statistics study of the s and t dependence of pp elastic and inelastic scattering as well as elastic and coherent inelastic pd scattering.

Scientific Spokesman: Stephen Olsen
716-275-4394
NAL Ext. 3795

Introduction

There has recently been a proposal by Jovanovic, Malamud, Nikitin and Kuznetsov to construct an experimental hall at C-O. To exploit the advantages offered by this new area we are here revising our proposal #198. The physics objectives, discussed in detail in our original proposal, are briefly restated here. By studying pp and pd elastic and inelastic scattering from 30 to 500 GeV in the $|t|$ range 0.3 to 5.0 GeV^2 we hope to find answers to the questions:

1. Does shrinkage persist at high t?
2. How does the break in the elastic differential cross section at 30 GeV develop into the dip observed at the ISR?
3. Does the position of the dip vary with energy?
4. What is the s dependence of $d\sigma/dt$ for t's beyond the dip?
5. Is there structure similar to that for elastics in the inelastic production of nucleon isobars?
6. What is the x and s dependence of the inclusive proton spectrum near the kinematic limit? In the context of the triple Regge model, what is the strength of the triple-pomeron coupling? To determine this one needs to measure both x and s dependence.
7. How do coherent inelastic processes on deuterium compare with elastic pd scattering?

Competing Experiments at NAL

There are two other experiments at NAL studying elastic scattering at "high" t:

1. NAL #7 (Meson Laboratory)

This experiment will use a double arm spectrometer in a secondary beam. The expected counting rate is 20 events/day for a cross section of 100 nano-barns so the data rate in the region $|t| > 1$ GeV^2 may be marginal.

2. NAL #177 (Proton Laboratory)

Elastic pp scattering will also be measured at higher momentum transfers ($|t| \geq 5$ (GeV/c)^2). This experiment, also using two arms, will have high luminosity and will be sensitive to small cross sections. On the other hand, it will be difficult for this experiment to reach lower $|t|$ values. For example, at 400 GeV/c an event with $|t| \simeq 1$ (GeV/c)^2 will have a forward scattering angle of 2.5 mrad - a difficult particle to detect.

Since the dip in the elastic differential pp cross section occurs in the region $1 < |t| < 2$ GeV^2, neither of these experiments is well suited to study this structure.

Unique Advantages of the Internal Jet Target

The jet target has unique characteristics which make it especially well suited for the physics we have proposed to investigate. These properties include:

1. Low density target permitting good mass resolution.
2. High luminosity permitting high statistics.
3. Continuous energy variation of the incident beam during the machine ramp permitting study of the energy dependence of the processes studied.

In addition to these properties which are conducive to a good experiment, the jet target has the practical advantage that it is essentially parasitic in nature. Experiments in the internal target lab will not affect the experimental programs being carried out in the external beam lines.

3. Experiment #198 (Internal Target Laboratory)

In contrast to experiments #7 and #177, the proposed experiment #198 does not detect forward going particles but uses a single arm to detect the recoil proton. The separation of elastic and inelastic events therefore relies on an accurate determination

of the missing mass going forward.. Good mass resolution is in turn dependent on a precise determination of the recoil angle and the recoil momentum of the detected particle. A detailed calculation of our mass resolution is presented later. Here we outline the principal features of this problem and the general design of our single arm spectrometer.

The spectrometer is shown in Fig. 1. We will use two bending magnets which give a total $\int B \cdot dl$ of 50 kg-m and bend 3 GeV/c particles by 30° in the horizontal plane. Six vertical and 3 horizontal proportional wire chambers will measure the recoil angle and momentum. The forward chambers which measure the polar angle will consist of pairs of planes with 1 mm wire spacing "staggered" by 0.5 mm to give an effective spacing of 0.5 mm. Pions will be rejected by time-of-flight and a plastic Čerenkov counter at low momenta and by a gas Čerenkov counter at high momenta.

We will build two different "front ends" for the spectrometer. These are illustrated in Figs. 2a and 2b. The first (Fig. 2a) is a standard set-up consisting of wire planes separated by helium bags. The second (Fig. 2b) is a "zero mass" and therefore "zero multiple scattering" system consisting of a "slit" defined by veto counters inside machine vacuum which is extended $\sim$5m to the first magnet. In this system we trade off counting rate for high resolution.

The Multiple Scattering Problem

The accuracy to which recoil angles and momenta can be measured can be no better than the limits imposed by multiple Coulomb scattering. There is no way to avoid this - the best we can hope to do is to reduce the multiple scattering to the point where its contribution is acceptable. Multiple scattering in a conventional liquid hydrogen target typically limits the mass resolution at 300 GeV incident energy to $\sim$1 GeV/c^2 which is not good enough to separate elastic and inelastic events.

In comparison, the largest contributions to multiple scattering using a gas jet target come from the vacuum exit window and the detectors. In our set-up of Fig. 2a these contributions can be reduced to the point where $\Delta M \simeq \pm 240$ MeV/c^2 at 400 GeV incident energy and $|t| = 1.5$ GeV^2. We can improve considerably on this resolution by eliminating entirely the effects of multiple scattering in our measurement of the polar angle. This can be done by extending the machine vacuum up to the first magnet as shown in Fig. 2b. Two small plastic scintillators in vacuum $\sim$1 m from the target define a 1 mm wide "slit" by vetoing all particles not passing through the slit. A second position measurement is made with a wire plane immediately behind the vacuum exit window which is 5 m from the target. The angle measurement, having been made essentially in vacuum, is independent of any multiple scattering and its accuracy depends only on the slit size and wire spacing. Indeed, the accuracy is so good, $\Delta\theta \simeq \pm 0.1$ mr, that the incident beam divergence becomes non-negligible.

With the "slit" arrangement of Fig. 2b we obtain a mass resolution of $\Delta M \simeq \pm 135$ GeV/c^2 at 400 GeV incident energy and $t \simeq -1.5$ GeV^2. The price for this improved resolution is a reduction in counting rate by a factor 30 from that of the conventional wire plane system of Fig. 2a.

Resolution Calculations

The limiting factor in the mass resolution of the proposed spectrometer is multiple Coulomb scattering in the vacuum window and wire planes. We minimize the path through air by placing helium bags between the chambers and inside the magnets.

Fig. 2a shows the thicknesses of material through which the scattered protons pass. The most critical window is the one separating machine vacuum from atmosphere. In Exp. 188 (Rutgers - I.C.) we used a 3-mil titanium window which was bench tested to destruction and broke at 450 psi, i.e. 30 atmospheres. 3-mil H-

film (mylar) windows were also tested and found to hold up to 10 atmospheres. For the present experiment we plan to use 3-mil H-film backed up by an isolation gate valve so that the H-film window would see machine vacuum only during data-taking. If the accelerator section judged the H-film window too thin to use over long periods, we would begin with a Ti window.

As an example we calculate the mass resoltuion at $t = -1.5$ GeV^2, the region of the dip in the elastic cross section. The recoil momentum at this t is $p \simeq 1.5$ GeV/c. Using the arrangement of Fig. 2a with a 3-mil H-film vacuum window we get an uncertainty in the polar angle of $\Delta\theta = \pm 0.37$ mr. The uncertainty in the angle of bend through the magnet is $\Delta\phi = \pm 0.39$ mr. For a 30^o bend this corresponds to $\Delta p/p = \pm 0.76 \times 10^{-3}$. Multiplying these uncertainties by $\partial M/\partial\theta$ and $\partial M/\partial p$ and adding quadratically we obtain a mass resolution of ±240 MeV at 400 GeV incident energy. Included in $\Delta\theta$ and $\Delta\phi$, in addition to multiple scattering effects, are measurement errors due to wire spacing. The incident beam divergence is included in $\Delta\theta$. The effect of the uncertainty in the incident beam momentum is very small and has been neglected.

Our mass resolutions at 400 GeV are summarized in Table I. Since the mass resolution is a linear function of the incident energy E, resolutions at energies other than 400 GeV may be obtained by multiplying the values of Table I by E/400.

TABLE I. The mass resolution, in MeV, of the wire plane (Fig. 2a) and slit (Fig. 2b) spectrometers at 400 GeV incident energies. Mass resolutions at energies E other than 400 GeV can be obtained by multiplying the given resolutions by E/400.

t(GeV^2)	Mass Resolution (MeV) Wire Chambers (Fig. 2a)	Mass Resolution (MeV) Slit System (Fig. 2b)
-0.5	±335	±150
-1.5	±240	±135
-4.0	±190	±125
-10.0	±215	±200

Counting Rates and Backgrounds

In the region of the break ($t \simeq -1.5$ GeV^2) we expect the elastic rate for 5×10^{12} protons/pulse to be

$$N_{el} = L\, d\sigma/dt\, \Delta t\, \Delta\phi/2\pi$$

$$= 10^{34} \times 10^{-31} \times 0.2 \times 0.02/2\pi$$

$$= 0.6/\text{machine pulse}$$

where L is the luminosity. This is the expected rate for the large solid angle system shown in Fig. 2a. For the slit system (Fig. 2b) the rate is a factor 30 lower.

Although the elastic events occur at the kinematic limit, due to the finite acceptance of the spectrometer (at $t = -1.5$ GeV^2, $\Delta\Omega\, \Delta p = 5 \times 10^{-3} \times 0.15$ GeV/c) we will be sensitive to legitimate (reconstructable) inelastic events. We estimate the number of inelastic events will be a factor $\sim$10 greater than the number of elastic events. The lower limit on the trigger rate will therefore be $\sim$10 greater than the elastic rate. Although the upper limit on the trigger rate is difficult to estimate, we feel it should not be too much higher since all spectrometer elements are well inside the enlarged C-O "alcove" and therefore well shielded from all but beam-target interactions.

Event rates for our studies of $pp \rightarrow pX$ and $pD \rightarrow pD$, as calculated in our original proposal #198, will typically be $\sim 10^3$/machine pulse.

From measurements made during E188 we estimate the singles rate in our first wire chamber (two meters from the target) to be $\sim$1 Mc which leads to a 10% probability of having two wires fire during the 100 ns resolving time of the chamber. The probability of "doubles" in the chambers further from the target will be much less and we will isolate real from spurious tracks by using the large degree of redundancy provided by our six chambers.

At recoil momenta below 2 GeV/c protons are ~3.5 ns slower than π's over the length of the spectrometer and we will use time-of-flight (using RF signal) together with a "Fitch" type lucite Čerenkov counter to separate p's from π's. Above 2 GeV/c we will use a gas Čerenkov counter.

Summary

The arguments presented in this proposal lead to the conclusion that the internal target laboratory is the only area at NAL in which the proposed physics objectives can be adequately carried out. The unique properties of the laboratory, i.e., a thin target due to the gas jet coupled with high luminosity due to multiple traversals of the incident beam, make possible both a high resolution and a high statistics experiment. The other obvious advantage of the laboratory is the availability of a variable energy incident beam and the possibility of extending the measurements immediately to any higher energies that may become available.

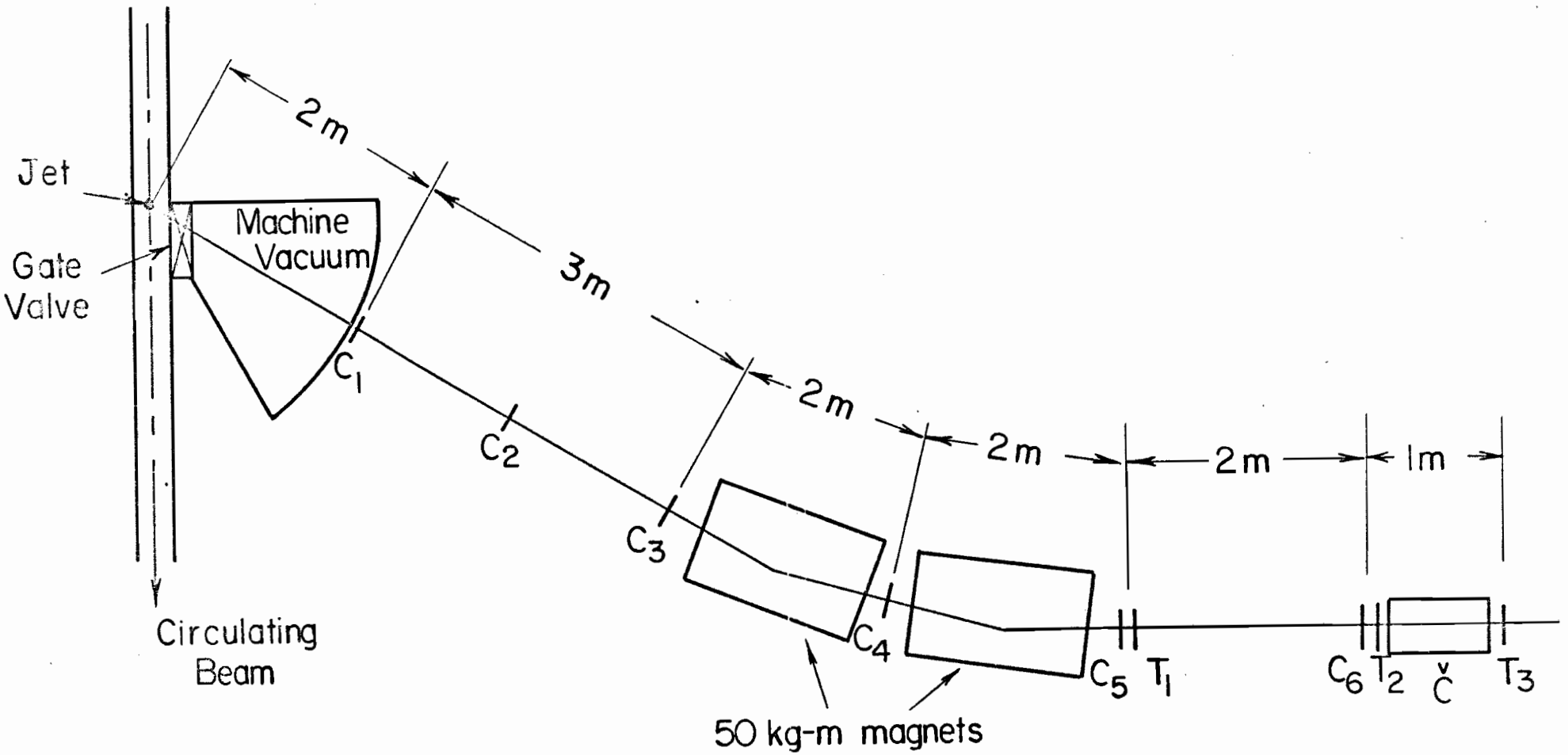

Fig. 1.

Fig. 1. The spectrometer set-up inside an enlarged C-O area. The C's denote multi-wire proportional chambers and the T's denote plastic trigger counters. Included in the trigger will be an RF signal. Helium bags are used between all elements and inside the magnets.

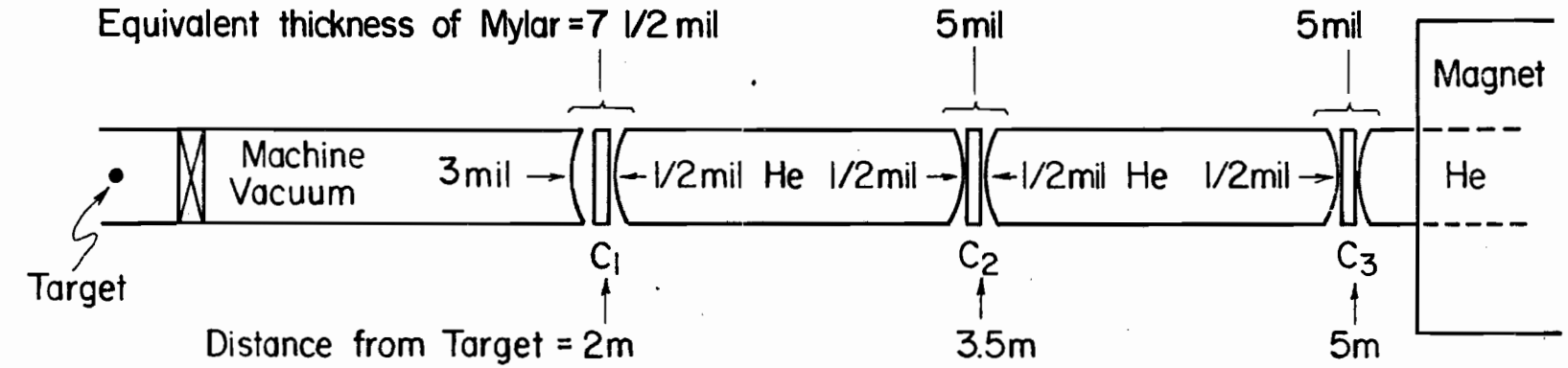

Fig 2 a.) (Elevation)

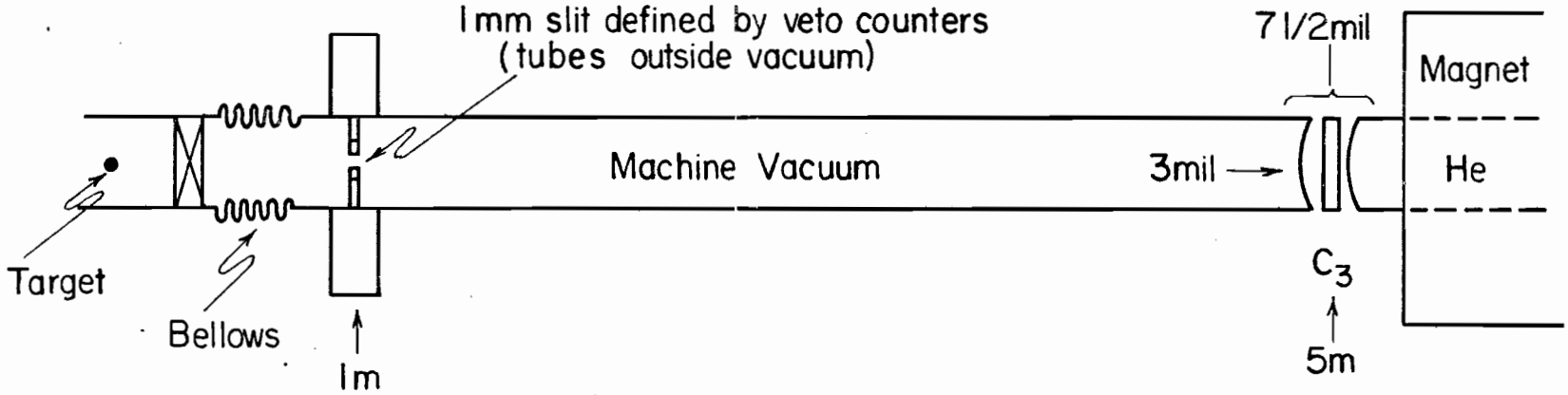

Fig 2 b.) (Plane View)

Fig. 2. Two variations of the "front end" of the spectrometer of Fig. 1. Fig. 2a is the conventional, high rate wire chamber system. Fig. 2b is the high resolution "slit" system.